Queues with Delayed Information: A Dynamical Systems Perspective

Faouzi Lakrad
Laboratory of Renewable Energy and Dynamics of Systems
Faculty of Sciences Ain Chock
Université Hassan II Casablanca
faouzi.lakrad@univh2c.ma

Jamol Pender
School of Operations Research and Information Engineering
Cornell University
228 Rhodes Hall, Ithaca, NY 14853
jjp274@cornell.edu

Richard Rand
Department of Mathematics
Sibley School of Mechanical and Aerospace Engineering
Cornell University
417 Upson Hall, Ithaca, NY 14853
rand@math.cornell.edu

April 26, 2020

Abstract

In this paper, we consider an N-dimensional queueing model where customers join according to a multinomial logit choice model. However, we assume that the information that the customer receives about the queue length is delayed by a constant Δ. We review how a large customer scaling of the stochastic model yields a system of delay differential equations. We also show how these limiting delay differential equations approximate the stochastic mean dynamics of the original queueing model. To gain insight about the queue length dynamics such as the amplitude, frequency, and the value of the critical delay we use the harmonic balance method and the method of multiple scales. We show that the method of multiple of scales is more accurate, however, is less tractable from a computational perspective than the harmonic balance method. Using the method of multiple scales, we also prove that the only stable mode

is where all N queues have the same amplitude and frequency, however, each queue is shifted by $\frac{2\pi}{N}$ from its neighbor. This analysis provides great insights for queues with delayed information and how the oscillations manifest themselves.

1 Introduction

Technology has allowed customers to get unprecedented access to information. One example of this information is delay announcements, which allow customers to receive an estimated waiting time until they are served. As a result, there is tremendous value in understanding the impact of providing waiting time or queue length information to customers. These announcements can affect the decisions of customers as well as the queue length dynamics of the system. Thus, the development of methods to support such announcements and interaction with customers has attracted the attention of the operations research and applied mathematics communities and is growing steadily.

Delay announcements are useful tools for managers of call centers and service systems to be able to interact and notify customers of their expected waiting time. The majority of the literature in queueing theory that analyzes delay announcements tends to focus on the impact of delay announcements on customer abandonment. For the most part, the literature only explores how customers respond to the delay announcements and also assumes that there is only one potential queue to join. Previous work by Armony and Maglaras [3], Avramidis and L'Ecuyer [6], Guo and Zipkin [9], Hassin [12], Armony et al. [4], Guo and Zipkin [10], Jouini et al. [17, 18], Allon and Bassamboo [1], Allon et al. [2], Ibrahim and Whitt [14], Thiongane et al. [34], Jennings and Pender [16], Thiongane et al. [35], Ibrahim et al. [15], Whitt [37], Bassamboo and Ibrahim [7], Ibrahim [13], Shah et al. [31], Thiongane et al. [36] and references therein focus on this aspect of the announcements. Thus, previous work does not focus on the situation where the information given to customers in the form of an announcement is delayed and how this delay in information can affect the dynamics of the underlying service.

Only recently has there been work that considers queues with delayed information that is not written by the authors. One paper that arises is the work of Lipshutz and Williams [20]. In this paper, the authors derive sufficient conditions for when oscillations will occur in reflected delay differential equations when they are present in the non-reflected differential equations. Since our work is based on the infinite server queue, our work does not consider the impact of reflections on the delay differential equations, which is a very difficult problem. One other major difference is that our queueing model is multi-dimensional while the model in Lipshutz and Williams [20] is one-dimensional. This is mainly because in the reflected delay differential equation setting, the reflections can be of many types and this cause tremendous technical difficulties. Finally, we are interested in computing exactly where the Hopf bifurcation occurs, while Lipshutz and Williams [20] does not compute exactly when this bifurcation will occur in the reflected model. A second paper is by Raina and Wischik [29]. This paper uses Lindstedt's method to compute the amplitude of oscillations for sizing router buffers in Internet infrastructure services. However, they do not compute closed form expressions for the amplitude and only provide numerical examples in this regard.

Recent work by the authors also considers queues with delayed information Pender et al.

[26, 27], Novitzky et al. [25, 24], Nirenberg et al. [23]. As a result, we need to explain how our current work in this paper differs from the previous literature on the topic. However, what makes this particular work different is that in this paper, we consider in full context the N dimensional queueing model. We show using harmonic balance that the steady state oscillations can be described by sinusoidal functions that are each shifted by the roots of unity. Previous work such as Pender et al. [26, 27] has only explored the two dimensional case and did not analyze the amplitude of oscillations. Previous work such as Novitzky et al. [25, 24] do study the amplitude of oscillations, but restrict the analysis to the two dimensional case. In fact the two dimensional case is much easier than the N dimensional setting since a reduction can be made to a one dimensional problem, which has an explicit solution. The N dimensional problem needs a more refined analysis because it theoretically involves 3-dimensional tensors. Finally, recent work such as Pender et al. [28], Nirenberg et al. [23] analyze stochastic versions of the queueing system and try to understand the impact of delayed information in the stochastic setting. They find that the stochastic fluctuations can have a large impact on the oscillations generated by the Hopf bifurcation in the deterministic model. However, this work does not give a detailed analysis of the delay differential equations that result from the limit theorems as we do here.

Figure 1.1: Disney waiting times on smartphone app, displayed in List (left) and Map (right) Forms.

One practical application of our work is for amusement parks like Disneyland or Six Flags. In Figure 1.1, we show a snapshot of the Disneyland app. The Disneyland app lists waiting times and the rider's current distance from each ride in the themepark. Customers obviously have the opportunity to choose which ride that they would want to go on, however, this choice depends on the information that they are given through the app. However, the

wait times on the app might not be posted in real-time or customers might need travel time to get to their next ride, the information they make their decision on is essentially delayed. Thus, our queueing analysis is useful for Disney to understand how their decision to offer an app that displays waiting time information will affect the lines for rides in the park.

Other applications of our work includes healthcare systems and urban transportation networks. Recently, many healthcare providers have started to post their waiting times and queue lengths online, highway billboards, and even through apps Dong et al. [8]. This has a large impact on where patients will choose to receive care since they want their wait to be short. This type of load balancing is also be used in NYC during the COVID-19 pandemic where patients are moved from crowded hospitals to less crowded hospitals. In this case, the delay can be viewed as the travel time of a moved patient.

In the context of transportation, many systems such as scooter and bike sharing networks provide riders with information about the availability of scooters and bikes. However, due to data processing, the information that riders receive is delayed in most systems by one minute Tao and Pender [32, 33]. Also in the context of transportation, many road networks provide information about a particular route and this information is often not given in real time. Thus, delayed information has a large impact on our society and it is really important to understand the effects of delaying information to large populations.

This paper introduces a stochastic queueing model, which describes the dynamics of customer choice with delayed information. In the queueing model, the customer receives information about the queue length which is delayed by a constant parameter Δ. Our goal in this work is not to prove that the stochastic model converges to the system of delay differential equations, but instead to show how the methods of harmonic balance and multiple scales can be used to uncover important insights about the limits of the stochastic queueing model. Using these two methods we are able to show that the dynamics of the fluid limit depend enormously on the initial functions used to start the delay differential system. Moreover, we find that the only stable mode of dynamics is one where all queues have the same amplitude and frequency, however, each is shifted by the roots of unity i.e. $\frac{2\pi}{N}$. Our analysis combines theory from delay differential equations, customer choice models, stability analysis of differential equations, and asymptotic analysis.

1.1 Main Contributions of Paper

The contributions of this work can be summarized as follows:

- Accurate analytical expressions of N queues length limit cycles using the harmonic balance method and the multiple scales method. Our analysis of the N-dimensional case represents a significant advance over the two dimensional case since it involves a "difference" analysis and tensor analysis. The two dimensional case has a symmetry that reduces it to a one dimensional problem, which is not present in our higher dimensional problem.

- We show that the system of N delay differential equations depends on the initial function in a very important way. If any of the equations are initialized with the same function, then they will remain the same throughout, which changes the dynamics. However, if all equations are initialized with different values, then the steady state

solution when $\Delta > \Delta_c$ is given by periodic function, having the same amplitude and frequency and they are equally shifted by the phase angle $\frac{2\pi}{N}$.

- We show when $\Delta > \Delta_c$, the amplitude of oscillations is increasing with increasing the time delay and the rate of this increase is lowered when the number of queues increases. Moreover, when $\Delta > \Delta_c$, the frequency of oscillations is decreasing with increasing the time delay and the rate of this decrease is lowered when the number of queues increases.

1.2 Organization of Paper

The remainder of this paper is organized as follows. Section 2 describes a constant delay fluid model. We derive the critical delay threshold under which the queues are balanced if the delay is below the threshold and the queues are asynchronized if the delay is above the threshold. In Section 3, we analyze the N-dimensional dde system. We calculate an explicit expression for the critical delay and frequency for our queueing model. We make a connection to the Lambert-W function and show how a clever reduction can simplify our analysis. In Section 4, we describe the harmonic balance method and apply it to our queueing problem. We show to derive a first order approximation of the queue length amplitude, frequency, and phase shift using harmonic balance. In Section 5, we describe the method of multiple scales and apply it to our problem. Using the method, we show that the only stable mode is one where all queues are sinusoidal functions that are shifted by the roots of unity from their neighbor. In Section 6, we conclude with directions for future research related to this work. Finally, we provide the proofs of our results in the Appendix.

2 The Queueing Model

In this section, we present a new stochastic queueing model with customer choice based on the queue length with a constant delay. Thus, we begin with N infinite-server queues operating in parallel, where customers make a choice of which queue to join by taking the size of the queue length into account via a customer choice model. We assume that the total arrival rate to the system (sum of all queues) is λ and the service rate at each queue is given by μ. However, we add the twist that the queue length information that is given to the customer is delayed by a constant Δ for all of the queues. Therefore, the queue length that the customer receives is actually the queue length Δ time units in the past.

Since customers will decide on which queue to join based on the queue length information, the choice model that we use to model the choice that the customers chooses dynamics is identical to that of a generalized Multinomial Logit Model (MNL). Thus, in a stochastic context with N queues, the probability of going to the i^{th} queue is given by the following expression

$$p_i(\mathcal{Q}(t), \Delta) \;=\; \frac{e^{-\gamma \mathcal{Q}_i(t-\Delta)}}{\sum_{j=1}^{N} e^{-\gamma \mathcal{Q}_j(t-\Delta)}} \tag{2.1}$$

where $\mathcal{Q}(t) = (\mathcal{Q}_1(t), \mathcal{Q}_2(t), ..., \mathcal{Q}_N(t))$. In this choice model, the parameter γ represents the sensitivity of customers to the queue length. The larger γ is, the more likely a customer is to join the shortest queue. In fact, if one sends $\gamma \to \infty$, then the choice function converges to the join the shortest queue function.

It is evident from the above expression that if the queue length in station i is larger than the other queue lengths, then the i^{th} station has a smaller likelihood of receiving the next arrival. This decrease in likelihood as the queue length increases represents the disdain customers have for waiting in longer lines. We should also mention that the MNL model we present in this work can be viewed as smoothed and infinitely differentiable approximation of the join the shortest queue model. Using these probabilities for joining each queue allows us to construct the following stochastic model for the queue length process of our N dimensional system for $t \geq 0$

$$\mathcal{Q}_i(t) = \mathcal{Q}_i([-\Delta, 0]) + \Pi_i^a \left(\int_0^t \frac{\lambda \cdot e^{-\gamma \mathcal{Q}_i(s-\Delta)}}{\sum_{j=1}^N e^{-\gamma \mathcal{Q}_j(s-\Delta)}} ds \right) - \Pi_i^d \left(\int_0^t \mu \mathcal{Q}_i(s) ds \right) \quad (2.2)$$

where each $\Pi(\cdot)$ is a unit rate Poisson process, $\mathcal{Q}_i([-\Delta, 0])$ is the initial function that sets $\mathcal{Q}_i(s) = \varphi_i(s)$ for all $s \in [-\Delta, 0]$ where $\varphi_i(s)$ is a Lipschitz continuous function. In this model, for the i^{th} queue, we have that

$$\Pi_i^a \left(\int_0^t \frac{\lambda \cdot e^{-\gamma \mathcal{Q}_i(s-\Delta)}}{\sum_{j=1}^N e^{-\gamma \mathcal{Q}_j(s-\Delta)}} ds \right) \quad (2.3)$$

counts the number of customers that decide to join the i^{th} queue in the time interval $(0, t]$. Note that the rate depends on the queue length at time $t - \Delta$ and not time t, hence representing the lag in information. Similarly

$$\Pi_i^d \left(\int_0^t \mu \mathcal{Q}_i(s) ds \right) \quad (2.4)$$

counts the number of customers that depart the i^{th} queue having received service from an agent or server in the time interval $(0, t]$. However, in contrast to the arrival process, the service process depends on the current queue length and not the past queue length.

2.1 Fluid Limits and Convergence

In many service systems, the arrival rate of customers is high. For example in Disneyland there are thousands of customers moving around the park and deciding on which ride they should join. Motivated by the large number of customers, we introduce the following scaled queue length process by a parameter η

$$\mathcal{Q}_i^\eta(t) = \mathcal{Q}_i^\eta([-\Delta, 0]) + \frac{1}{\eta}\Pi_i^a \left(\eta \int_0^t \frac{\lambda \cdot e^{-\gamma \mathcal{Q}_i^\eta(s-\Delta)}}{\sum_{j=1}^N e^{-\gamma \mathcal{Q}_j^\eta(s-\Delta)}} ds \right) - \frac{1}{\eta}\Pi_i^d \left(\eta \int_0^t \mu \mathcal{Q}_i^\eta(s) ds \right) \quad (2.5)$$

Note that we scale the rates of both Poisson processes, which is different from the many server scaling, which would only scale the arrival rate. Scaling only the arrival rate would

yield a different limit than the one analyzed by Pender et al. [26] since the multinomial logit function is not a homogeneous function. Moreover, one should observe the term $Q_i^\eta([-\Delta, 0])$, which highlights an important difference between delayed systems and their real-time counterparts. $Q_i^\eta([-\Delta, 0])$ is a necessary function that keeps track of the past values of the queue length on the interval $[-\Delta, 0]$. Unlike the case when $\Delta = 0$, we need more than an initial value $Q_i^\eta(0)$ to initialize our stochastic queue length process. In fact in the delayed setting, we need an initial function to initialize our stochastic queue length process. We need these values since our arrival rate function is delayed and depends on previous queue length information. By letting the scaling parameter η go to infinity, we obtain our first result.

Theorem 2.1. *Let $\varphi_i(s)$ be a Lipschitz continuous function that keeps track of the previous values on the interval $[-\Delta, 0]$. Then, if $\mathcal{Q}_i^\eta(s) \to \varphi_i(s)$ almost surely for all $s \in [-\Delta, 0]$ and for all $1 \leq i \leq N$, then the sequence of stochastic processes $\{\mathcal{Q}^\eta(t) = (\mathcal{Q}_1^\eta(t), \mathcal{Q}_2^\eta(t), ..., \mathcal{Q}_N^\eta(t)\}_{\eta \in \mathbb{N}}$ converges almost surely and uniformly on compact sets of time to $(q(t) = (q_1(t), q_2(t), ..., q_N(t))$ where*

$$\dot{q}_i(t) = \lambda \cdot \frac{e^{-\gamma q_i(t-\Delta)}}{\sum_{j=1}^N e^{-\gamma q_j(t-\Delta)}} - \mu q_i(t), \tag{2.6}$$

$q_i(s) = \varphi_i(s)$ for all $s \in [-\Delta, 0]$ and for all $1 \leq i \leq N$.

Proof. See Pender et al. [28] for the proof of this result. □

Theorem 2.1 states that as we let η go towards infinity, the sequence of queueing processes converges to a system of **delay differential equations**. Unlike ordinary differential equations, the existence and uniqueness results for delay differential equations is much less well known. However, we provide the result of existence and uniqueness for the delay differential system that we analyze in this paper below.

Theorem 2.2. *Given a Lipschitz continuous initial function $\varphi_i : [-\Delta, 0] \to \mathbb{R}$ for all $1 \leq i \leq N$ and a finite time horizon $T > 0$, there exists a unique Lipschitz continuous function $q(t) = \{q(t)\}_{-\Delta \leq t \leq T}$ that is the solution to the following delay differential equation*

$$\dot{q}_i(t) = \lambda \cdot \frac{e^{-\gamma q_i(t-\Delta)}}{\sum_{j=1}^N e^{-\gamma q_j(t-\Delta)}} - \mu q_i(t) \tag{2.7}$$

and $q_i(s) = \varphi_i(s)$ for all $s \in [-\Delta, 0]$ and for all $1 \leq i \leq N$.

Proof. The proof of this result can be found in Hale [11]. □

2.2 Understanding Through Numerical Examples

For the numerical integration, we use the dde23 solver under Matlab and ideas from L.F. and S. [19]. For all numerical integrations of Eq. 2.7, unless stated otherwise, we set $\lambda = 10$, $\mu = 1$ and $\gamma = 1$. Table 1 provides the critical time delays $\Delta_{c,N}$ and the equilibria q_N^s corresponding to N queues, where the integer $N = 2, ..., 7$.

Number of queues N	2	3	4	5	6	7
Critical time delay $\Delta_{c,N}$	0.362	0.590	0.865	1.209	1.661	2.300
Equilibrium q_N^s	5.00	3.33	2.50	2.00	1.67	1.43

Table 1: Critical time delays and equilibria for various number of queues

In Fig. 2.1 we show the time histories of the queue lengths in the case of four queues i.e. $N = 4$, for various time delays Δ and initial conditions. In Fig.2.1 (a), for $\Delta = 0.86 < \Delta_{c,4} = 0.865$ all the four queues lengths tend, in an oscillatory way, to the stable equilibrium $q_4^s = 2.5$. Figures 2.1(b), (c) and (d) show time histories of the four queues lengths for $\Delta = 0.88 > \Delta_{c,4}$ with various initial conditions. In Fig. 2.1(b), all four initial conditions are taken different, the four queues lengths are periodic with the same amplitude and period but they are identically shifted. In Fig. 2.1 (c) two queues lengths are initially identical, then three periodic solutions identically shifted with different amplitudes are obtained. In Fig. 2.1 (d) three queues lengths are initially identical. This case is similar to the case of two queues studied in Pender et al. [26]. The three identical queues are out of phase with the fourth queue. In Fig. 2.1(e), when all four queues are initially identical, the queue lengths are not oscillating and they converge very fast to the equilibrium q_4^s. These five figures show that the only stable solutions are given in Fig. 2.1(b), all the other cases are unstable since they are sensitive to initial conditions.

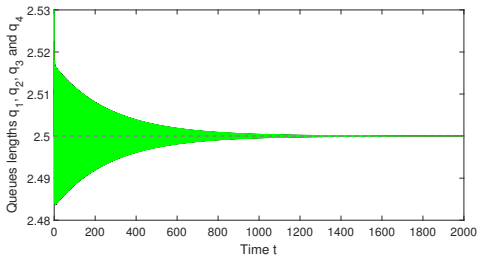

(a)$\Delta = 0.86$. For $t \in [-\Delta, 0]$: $q_1(t) = 2.5, q_2(t) = 2.51, q_3(t) = 2.52$ and $q_4(t) = 2.53$

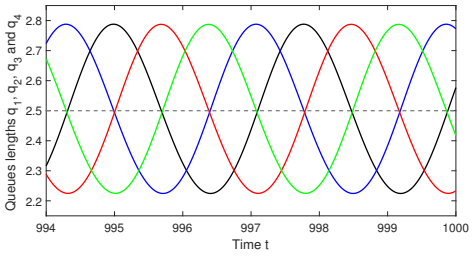

(b)$\Delta = 0.88$. For $t \in [-\Delta, 0]$: $q_1(t) = 1, q_2(t) = 1.1, q_3(t) = 1.2$ and $q_4(t) = 1.3$

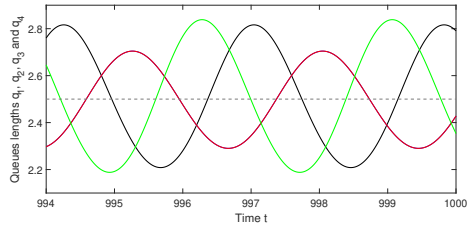

(c) $\Delta = 0.88$. For $t \in [-\Delta, 0]$: $q_1(t) = 1, q_2(t) = q_3(t) = 1.1$ and $q_4(t) = 1.2$

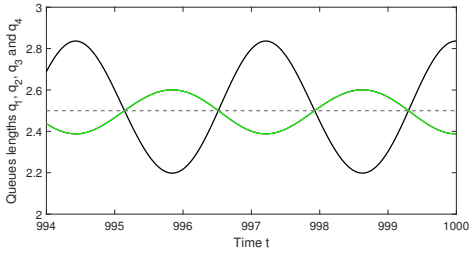

(d) $\Delta = 0.88$. For $t \in [-\Delta, 0]$: $q_1(t) = 1, q_2(t) = q_3(t) = q_4(t) = 1.1$

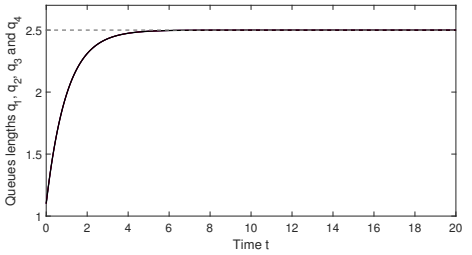

(e) $\Delta = 0.88$. For $t \in [-\Delta, 0]$: $q_1(t) = q_2(t) = q_3(t) = q_4(t) = 1.1$

Figure 2.1: Time histories of Eq.(2.7) for $N = 4, \gamma = 1$ for various time delays and for diverse initial conditions. $q_1(t)$ in black, $q_2(t)$ in blue, $q_3(t)$ in red and $q_4(t)$ in green. The dashed line corresponds to the equilibrium q_4^s.

Figure 2.2 shows, for various numbers of queues, the numerically computed amplitudes of the periodically oscillating queues lengths versus the time delay Δ. The amplitude increases with increasing the time delay above the critical value. Moreover, the increase rate of the amplitude is decreasing when the number N of queues increases, see Fig.2.2(b).
Figure 2.3 shows, for various numbers of queues, the numerically computed fundamental frequencies of the periodically oscillating queues lengths versus $\Delta - \Delta_{c,N}$. The fundamental frequency is decreasing with increasing the time delay Δ and it is decreasing with increasing the number N of queues. Moreover, the rate of frequency decrease is lower for higher numbers of queues. Consequently, the frequency of oscillations become slower as we increase the number of queues N.

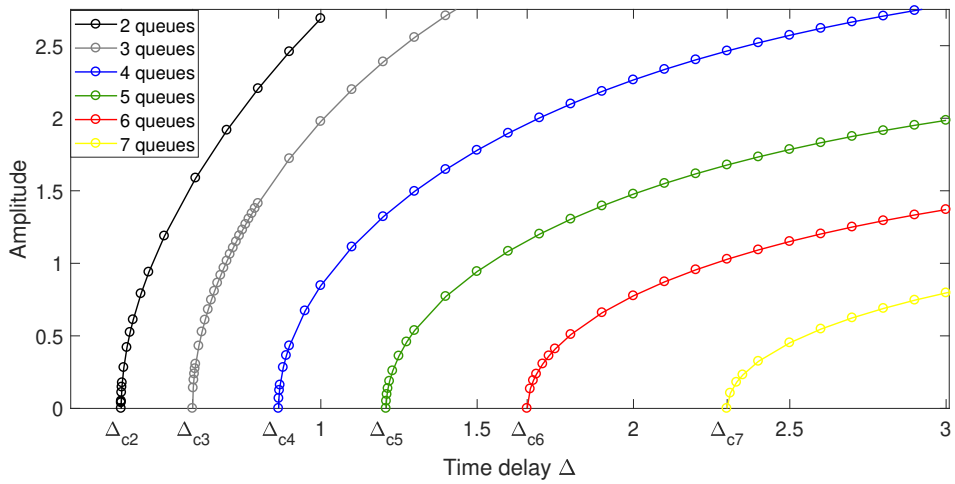

(a) Amplitudes versus the time delay Δ. Circles are the numerically computed amplitudes.

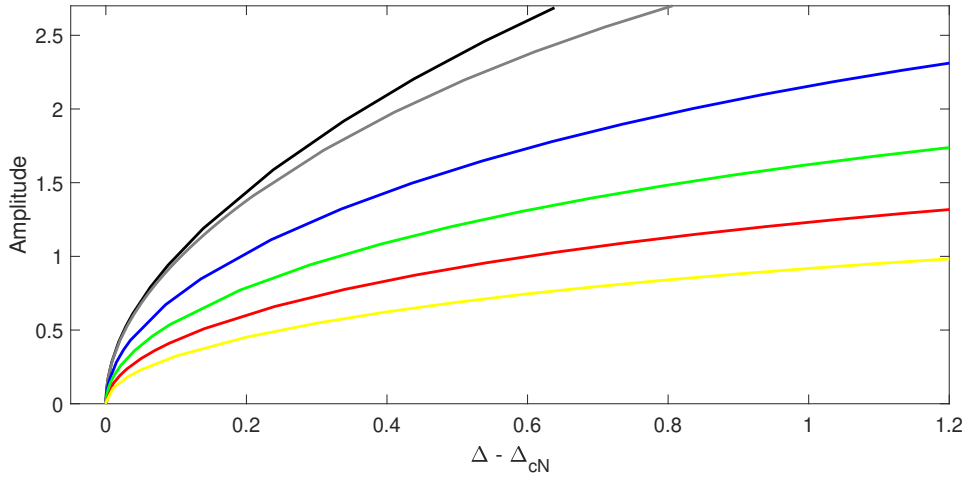

(b) Amplitudes versus $\Delta - \Delta_{c,N}$

Figure 2.2: Numerically computed amplitudes of $N = 2, 3, 4, 5, 6$ and 7 queues lengths versus $\Delta - \Delta_{c,N}$ the deviation of the time delay from its critical value

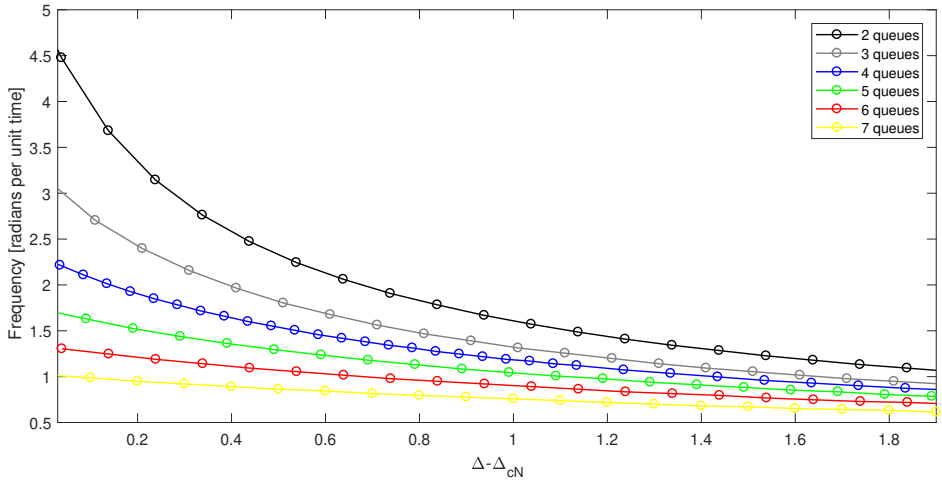

Figure 2.3: Numerically computed fundamental frequencies of various number of oscillating queues lengths versus $\Delta - \Delta_{c,N}$

3 Analysis of Delay Differential Equation Model

3.1 Model Reduction

The mathematical model of the queues lengths given in Eq.(2.7) depends explicitly on the sensitivity of customers to the queue length parameter γ. We will show in this subsection, through changes of variables, that the effect of γ can be reduced to a change of the total arrival rate. Thus, (wlog), we can assume $\gamma = 1$ for simplicity.
Setting $Q_n(t) = \gamma q_n(t)$ as the n^{th} new scaled queue length, then Eq.(2.7) becomes

$$\dot{Q}_n(t) = \Lambda \frac{\exp(-Q_n(t-\Delta))}{\sum_{k=1}^{N} \exp(-Q_k(t-\Delta))} - \mu Q_n(t), \qquad \text{where} \quad n = 1, ..., N. \tag{3.8}$$

where $\Lambda = \gamma\lambda$. Consequently, the exponential terms in Eq.(3.8) do not depend explicitly on γ. This latter changes the total arrival rate Λ to the system. It is worth noting that the sum of all scaled queues lengths $S(t) = \sum_{k=1}^{N} Q_k(t)$ is the solution to the following first order linear ordinary differential equation

$$\dot{S}(t) = \Lambda - \mu S(t). \tag{3.9}$$

3.2 An Equilibrium Analysis

Indeed Eq.(3.9) has one equilibrium $S^* = \Lambda/\mu$, and its solution is given by

$$S(t) = \frac{\Lambda}{\mu} + C \exp(-\mu t) \tag{3.10}$$

where C is a constant of integration. Consequently, the sum $S(t)$ tends asymptotically to the equilibrium S^*. The equilibrium of the n^{th} length queue Q_n^s is obtained by dropping the

time derivative in the left hand side of Eq.(3.8). It is solution of the following equation

$$\Lambda \frac{\exp(-Q_n^s)}{\sum_{k=1}^{N} \exp(-Q_k^s)} - \mu Q_n^s = 0, \qquad \text{where} \;\; n = 1, ..., N. \tag{3.11}$$

Since the equilibria of all queues obey the same equation in Eq. (3.11), then they are all equal. Using the fact that their sum is constant, they are given by

$$Q_n^s = Q^s = \frac{\Lambda}{N\mu}, \;\; \text{where} \;\; n = 1, ..., N. \tag{3.12}$$

3.3 Third Order Taylor Expansion

In order to use an analytical method to approximate solutions of the nonlinear delay differential equations (2.7) and (3.8), they are written in polynomial form using the Taylor expansion around the equilibrium. At least the third order Taylor expansion should be used, since the first and the second order expansions will give no information about the amplitude of the fundamental frequency. In fact, the first order expansion will give the critical time delay and the frequency of the born periodic solution. The second order expansion will give information about the amplitude of the first harmonic corresponding to twice the fundamental frequency. Furthermore, the quadratic and the cubic nonlinearities should be present in the truncated model in order to take into account the odd and the even nonlinearities present in the original DDEs. Admittedly, there is a trade-off between analytical tractability and the precision since the greater is the order of the used polynomials, the bigger is the validity domain and higher the precision of the truncated model.
The n^{th} queue length $Q_n(t)$ can be expressed as the following equation

$$Q_n(t) = Q^s + P_n(t) \tag{3.13}$$

where $P_n(t)$ is a perturbation around the equilibrium Q^s. Now by taking a Taylor expansion up to the third order, we obtain the following equation

$$\begin{aligned}
\dot{P}_n + \mu P_n + \frac{\Lambda}{N}\left(1 - \frac{1}{N}\right) P_{n\Delta} \;\; = \;\; & \frac{\Lambda}{N}\Bigg[\frac{1}{N}\sum_{\substack{k=1 \\ k\neq n}}^{N} P_{k\Delta} - \frac{1}{N}\sum_{k=1}^{N}\left(\frac{1}{2}P_{k\Delta}^2 - \frac{1}{6}P_{k\Delta}^3\right) \\
& + \;\; \frac{1}{N^2}\left(\sum_{k=1}^{N}(-P_{k\Delta} + \frac{1}{2}P_{k\Delta}^2)\right)^2 + \frac{1}{N^3}\left(\sum_{k=1}^{N} P_{k\Delta}\right)^3 \\
& + \;\; P_{n\Delta}\left(\frac{1}{N}\sum_{k=1}^{N}\left(-P_{k\Delta} + \frac{1}{2}P_{k\Delta}^2\right) - \frac{1}{N^2}\left(\sum_{k=1}^{N} P_{k\Delta}\right)^2\right) \\
& + \;\; \frac{1}{2}P_{n\Delta}^2\left(1 + \frac{1}{N}\sum_{k=1}^{N} P_{k\Delta}\right) - \frac{1}{6}P_{n\Delta}^3\Bigg].
\end{aligned} \tag{3.14}$$

One should note that Eq.(3.14) demonstrates the queues are coupled linearly and nonlinearly. The quadratic and cubic nonlinearities are proportional to N^{-2} and N^{-3}, respectively.

Consequently, the effect of nonlinearities and the coupling are weakening with increasing the number of queues N. In the limiting case $N \to +\infty$, the queues lengths equations are becoming linear and independent. Asymptotically the solutions are given by

$$\sum_{k=1}^{N} Q_k(t) = \frac{\Lambda}{\mu} \qquad \text{and} \qquad \sum_{k=1}^{N} P_k(t) = 0. \tag{3.15}$$

It should also be observed that the nonlinear couplings in Eq.(3.14) prevent the direct implementation of a perturbation technique to approximate the solutions. Hence, we define the J^{th} queue length as a reference and define its difference with respect to the n^{th} queue length as

$$D_n(t) = Q_J(t) - Q_n(t). \tag{3.16}$$

Consequently, $D_J(t) = 0$ and the N queues lead to $N-1$ queue lengths differences $D_n(t)$ with $n = 1, ..., N$ and $n \neq J$. Hence, the n^{th} queue length is the solution to the following delay differential equation

$$\dot{D}_n(t) = \Lambda \frac{1 - \exp(D_n(t-\Delta))}{1 + \sum_{\substack{k=1 \\ k\neq J}}^{N} \exp(D_k(t-\Delta))} - \mu D_n(t); \quad \text{where} \;\; J \neq n = 1, ..., N. \tag{3.17}$$

One observes now that Equation (3.17) has zero as an equilibrium solution. Using the Taylor series up to the third order around this trivial equilibrium solution, Eq.(3.17) becomes

$$\begin{aligned}
\dot{D}_n(t) &= \Lambda \Bigg[-\frac{1}{N} D_n(t-\Delta) + \left(\frac{2-N}{2N^2}\right) D_n^2(t-\Delta) + \frac{1}{N^2} D_n(t-\Delta) \sum_{\substack{k=1 \\ k\neq\{n,J\}}}^{N} D_k(t-\Delta) \\
&+ \left(\frac{-N^2+6N-6}{6N^3}\right) D_n^3(t-\Delta) + \left(\frac{N-4}{2N^3}\right) D_n^2(t-\Delta) \sum_{\substack{k=1 \\ k\neq\{n,J\}}}^{N} D_k(t-\Delta) \\
&+ \frac{1}{2N^2} D_n(t-\Delta) \Bigg(\sum_{\substack{k=1 \\ k\neq\{n,J\}}}^{N} D_k^2(t-\Delta) - \frac{2}{N} \left(\sum_{\substack{k=1 \\ k\neq\{n,J\}}}^{N} D_k(t-\Delta) \right)^2 \Bigg) \Bigg] - \mu D_n(t)
\end{aligned} \tag{3.18}$$

To the third order, the same results of Eq.(3.18) are obtained by using $D_n(t) = P_J(t) - P_n(t)$. Moreover, Eq.(3.18) contains only nonlinear coupling terms. In the special case of two queues i.e., $N = 2$, the equation of the lengths difference $D_2(t) = q_1(t) - q_2(t)$ is given by

$$\dot{D}_2 = \Lambda \left[-\frac{1}{2} D_2(t-\Delta) + \frac{1}{24} D_2^3(t-\Delta) \right] - \mu D_2(t), \tag{3.19}$$

this equation does not contain quadratic terms that break the symmetry of the problem. Consequently, the lengths of the two queues oscillate out of phase around the equilibrium with equal amplitudes. For more details see the work by Pender et al. [26].
Using Eqs. (3.15) and (3.16), the n^{th} modified queue length Q_n is given by

$$Q_n(t) = \frac{\Lambda}{N\mu} + \frac{1}{N} \sum_{k=1}^{N} D_k(t) - D_n(t), \quad \text{with} \;\; n = 1, ..., N. \tag{3.20}$$

3.4 Hopf bifurcation

The linear equations ruling the perturbation $P_n(t)$ and the difference $D_n(t)$ are deduced from Eqs. (3.14) and (3.18) as follows

$$\dot{P}_n + \mu P_n + \frac{\Lambda}{N} P_{n\Delta} = \frac{\Lambda}{N^2} \sum_{k=1}^{N} P_{k\Delta} \tag{3.21}$$

$$\dot{D}_n + \mu D_n + \frac{\Lambda}{N} D_{n\Delta} = 0. \tag{3.22}$$

The linear equations of the differences (3.22) are decoupled while equations of the deviations from the equilibrium (3.21) have the same coupling term. Moreover, Eq. (3.22) has $D = 0$ as an equilibrium solution that corresponds to $Q_n(t) = Q_J(t)$, $\forall\ n = 1, ..., N$. The linear stability of $D = 0$ is defined through solving the following transcendental characteristic equation

$$r + \mu + \frac{\Lambda}{N} e^{-r\Delta} = 0. \tag{3.23}$$

Equation (3.23) has an infinite number of complex solutions that can be expressed in terms of the k^{th} branch W_k of the Lambert function as follows

$$r_k = \frac{1}{\Delta} W_k(H) - \mu, \qquad \text{where } H = -\frac{\Lambda\Delta}{N} e^{\mu\Delta},\ k \in \mathbb{Z}. \tag{3.24}$$

Eq. (3.23) can have real roots, in the following cases

- If $H \neq 0$ or $H = e^{-1}$: Eq.(3.23) has one real root that is

$$r = -W_0(H) + \mu\Delta. \tag{3.25}$$

- If $H \in]-e^{-1}, 0[$: Eq.(3.23) has two real roots that are

$$r = -W_0(H) + \mu\Delta \qquad \text{and} \qquad r = -W_{-1}(H) + \mu\Delta. \tag{3.26}$$

- If $H < -e^{-1}$: Eq.(3.23) has no real root.

For more details about the application of the Lambert function for linear DDEs see Asl and Ulsoy [5].
In Fig.3.1 are shown the real and imaginary parts of 20 roots of the characteristic equation (3.23), in the case of $N = 4$ queues, for various values of the time delay Δ bellow and above the critical value $\Delta_{c,4} = 0.865$. In Figs. 3.1(a) and (b) the equilibrium $D = 0$ is stable and in the remaining figures it is unstable. The stability boundary of the equilibrium $D = 0$ is given by vanishing the real part of r and thus it becomes purely imaginary and can be expressed by $r = i\omega_c$. Then, separating the real and the imaginary parts of Eq.(3.23) leads to the following equations

$$\begin{cases} \mu + \frac{\Lambda}{N} \cos(\omega_c \Delta_c) = 0 \\ \\ \omega_c - \frac{\Lambda}{N} \sin(\omega_c \Delta_c) = 0. \end{cases} \tag{3.27}$$

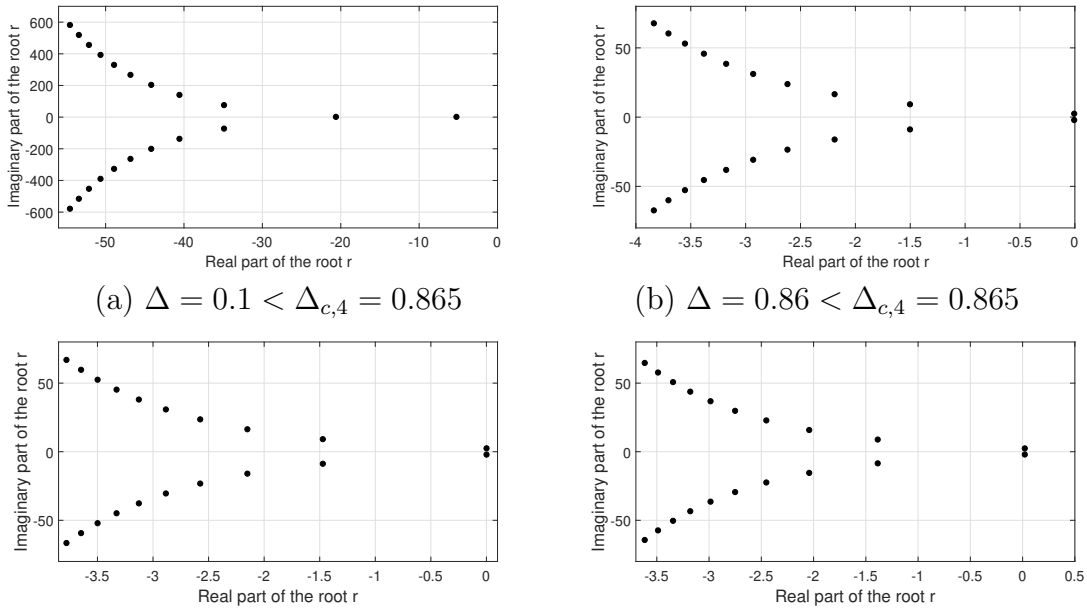

(a) $\Delta = 0.1 < \Delta_{c,4} = 0.865$ (b) $\Delta = 0.86 < \Delta_{c,4} = 0.865$

(c) $\Delta = 0.87 > \Delta_{c,4} = 0.865$ (d) $\Delta = 0.90 > \Delta_{c,4} = 0.865$

Figure 3.1: Twenty roots of the characteristic equation given in Eq. (3.23) for $N = 4$.

The existence of a real positive ω_c implies the birth of a periodic solution through a Hopf bifurcation and the instability of the $D = 0$ equilibrium. The frequency ω_c of the born periodic solution is given by

$$\omega_c = \sqrt{\left(\frac{\Lambda}{N}\right)^2 - \mu^2}. \tag{3.28}$$

The periodic solution exists if $\gamma\lambda/\mu > N$. When the number of queues N increases, the frequency ω_c of the born periodic solution is decreasing. The critical time delay Δ_c that causes this Hopf bifurcation is given by

$$\Delta_c = \frac{1}{\omega_c} \arccos\left(-\frac{\mu N}{\Lambda}\right) = \frac{N}{\sqrt{\Lambda^2 - N^2\mu^2}} \arccos\left(-\frac{\mu N}{\Lambda}\right). \tag{3.29}$$

Hence, if $\Delta < \Delta_c$ then the equilibrium $D = 0$ is stable otherwise it is unstable and a periodic solution is born. When the number of queues N increases the critical delay time Δ_c increases also. Moreover, Δ_c is decreasing with increasing Λ, λ or γ. Equations (3.27), (3.28) and (3.29) are also obtained by looking for a harmonic solution of two queues difference $D(t) = a_c \cos(\omega_c t)$ in equation (3.22). It is important to note that the linear analysis does not give any information on the amplitude a_c of the born periodic solution.

4 Harmonic Balance Method

In the previous section, it was shown that the system is undergoing a Hopf bifurcation and consequently the queues lengths are oscillating periodically and can be expressed in terms of a Fourier series. Hence, in order to obtain an analytic approximation of periodic solutions of Eq. 3.14, we will use the Harmonic Balance Method (HBM). This method approximates the queue length solution as a truncated Fourier series that contains only the highly contributing frequencies.

In order to quantify the contribution of the fundamental frequency and its harmonics to the periodic solution, their powers are computed and represented in the frequency domain. Mathematically, the power of a signal is proportional to the square of the modulus of its Fourier transform and here it is computed using a fast Fourier transformation algorithm.

In Fig. 4.1 we plot the numerical time histories and the corresponding power spectra of Eqs.(2.7) in the case of 4 and 7 queues, for time delays larger than the respective critical delay. The power spectra show that the fundamental frequency is the dominant contributor to the solution since the ratio of the power at the the fundamental frequency to the power at the first harmonic is equal to 776.5 for $N = 4$ and to 288 for $N = 7$. Several numerical integrations were performed for various numbers of queues and time delays and the fundamental frequency was all the time dominant. It is to be expected that the contribution of harmonics would increase slightly for increasing the difference between the time delays Δ and Δ_c. It should be noted that the frequency, in the power spectra plots, is number of queues lengths oscillations cycles per unit time and the frequency ω is expressed in radians per unit time.

4.1 Phase shifts of the born periodic solutions

First, we will apply the HBM to determine the phase shifts of the born periodic solutions through the Hopf bifurcation. For a given number of queues, the linear equation given in Eq. (3.21) of the queue length deviations from the equilibrium q^s are identical for all queues, thus the born periodic solutions are identical (the same amplitude a^* and the same frequency ω_c) up to a phase shift. The harmonic balance method is used to compute these phases shifts, the n^{th} queue deviation $P_n(t)$ is expressed as follows

$$P_n(t) = a^* \cos(\omega_c t - \phi_n) \tag{4.30}$$

Inserting the solution of Eq. (4.30) into Eq. (3.21) and equating terms in $\cos(\omega_c t)$ and $\sin(\omega_c t)$ leads to the following two equations

$$\cos(\phi_n)\Big[\mu + \frac{\lambda\gamma}{N}\cos(\omega_c\Delta_c)\Big] + \sin(\phi_n)\Big[\omega_c - \frac{\lambda\gamma}{N}\sin(\omega_c\Delta_c)\Big] = \frac{\lambda\gamma}{N^2}\sum_{k=1}^{N}\cos(\omega_c\Delta_c + \phi_k) \tag{4.31}$$

$$\sin(\phi_n)\Big[\mu + \frac{\lambda\gamma}{N}\cos(\omega_c\Delta_c)\Big] - \cos(\phi_n)\Big[\omega_c - \frac{\lambda\gamma}{N}\sin(\omega_c\Delta_c)\Big] = \frac{\lambda\gamma}{N^2}\sum_{k=1}^{N}\sin(\omega_c\Delta_c + \phi_k) \tag{4.32}$$

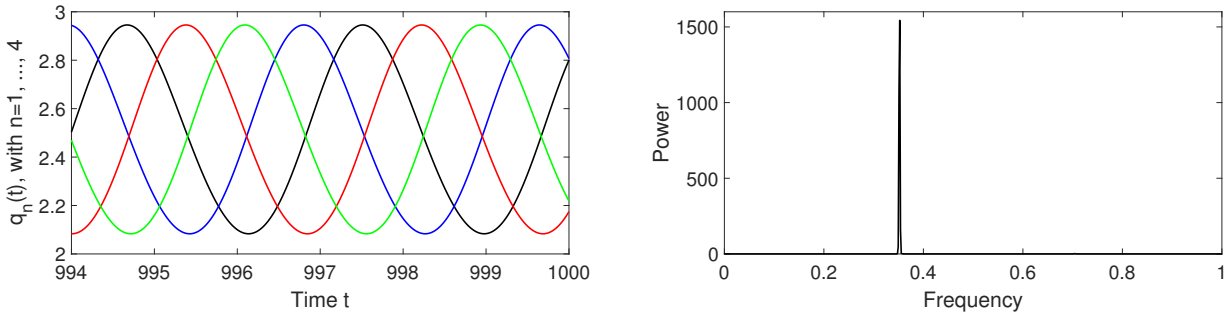

(a) Case $N = 4$ for $\Delta = 0.90 > \Delta_{c,4} = 0.865$

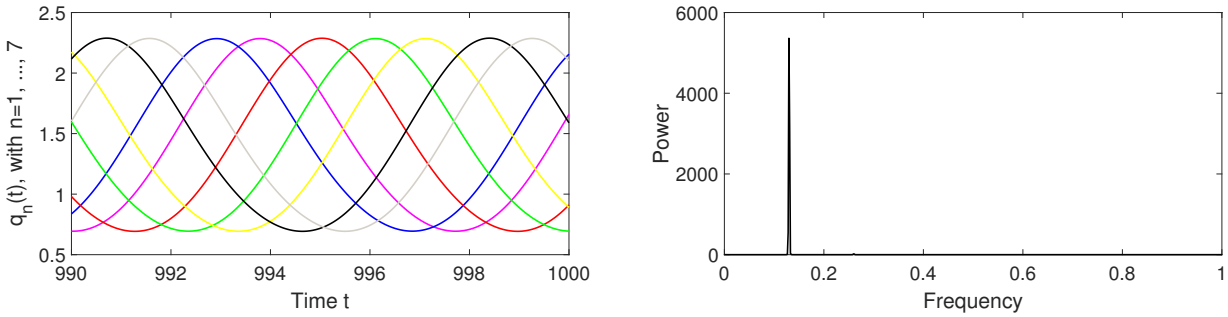

(b) Case $N = 7$ for $\Delta = 3 > \Delta_{c7} = 2.30$

Figure 4.1: Time histories and power spectra of Eq.(2.7) for $N = 4$ and $N = 7$.

Terms multiplied by $\cos(\phi_n)$ and $\sin(\phi_n)$ are equal to zero since they are the same as the terms of Eq.(3.27). Consequently,

$$\sum_{k=1}^{N} \cos(\omega_c \Delta_c + \phi_k) = 0 \qquad ; \qquad \sum_{k=1}^{N} \sin(\omega_c \Delta_c + \phi_k) = 0. \tag{4.33}$$

These two equations can be written as follows

$$\cos(\omega_c \Delta_c) \sum_{k=1}^{N} \cos(\phi_k) - \sin(\omega_c \Delta_c) \sum_{k=1}^{N} \sin(\phi_k) = 0 \tag{4.34}$$

$$\cos(\omega_c \Delta_c) \sum_{k=1}^{N} \sin(\phi_k) + \sin(\omega_c \Delta_c) \sum_{k=1}^{N} \cos(\phi_k) = 0. \tag{4.35}$$

Finally, phases shifts ϕ_k of the N queues are governed by the following two equations

$$\sum_{k=1}^{N} \cos(\phi_k) = 0 \qquad \text{and} \qquad \sum_{k=1}^{N} \sin(\phi_k) = 0. \tag{4.36}$$

Hence, the phase shifts between the N queues lengths are $\phi_k = 2k\pi/N$, with $k = 1, 2, ..., N$.

4.2 Amplitude and frequency of the periodic solution

In this subsection, an explicit expression of the periodic solutions of Eq. (3.14) are derived, using the HBM, beyond the Hopf bifurcation. Hence, the solutions are sought in the following form

$$P_n(t) = a\cos(\omega t - \phi_n) \tag{4.37}$$

here only one term of the Fourier series is used in order to have an explicit expression of the amplitude a and the fundamental frequency ω. Inserting Eq.(4.37) into Eq.(3.14) and equating terms of $\cos(\omega t)$ and $\sin(\omega t)$ leads to the following two equations

- Equation of $\cos(\omega t)$:

$$\begin{aligned}
&\omega\sin(\phi_n) + \mu\cos(\phi_n) + \frac{\Lambda}{N}\cos(\omega\Delta+\phi_n) = \frac{\Lambda}{N^2}\sum_{k=1}^{N}\cos(\omega\Delta+\phi_k)\\
+\;& a^2\Bigg[\frac{\Lambda}{8N^2}\sum_{k=1}^{N}\cos(\omega\Delta+\phi_k) - \frac{\Lambda}{N^3}\Big[\frac{N}{2}\sum_{k=1}^{N}\cos(\omega\Delta+\phi_k) + \frac{1}{4}\sum_{k=1}^{N}\sum_{j=1}^{N}\cos(\omega\Delta+2\phi_k+\phi_j)\Big]\\
+\;& \frac{\Lambda}{N^4}\Big[\sum_{i=1}^{N}\sum_{k=1}^{N}\sum_{j=1}^{N}\left(\frac{\cos(\phi_j-\phi_k)}{2}\cos(\omega\Delta+\phi_i) + \frac{\cos(\omega\Delta+\phi_j+\phi_k-\phi_i)}{4}\right)\Big]\\
+\;& \frac{\Lambda}{4N^2}\Big[N\cos(\omega\Delta+\phi_n) + \sum_{k=1}^{N}\cos(\omega\Delta+2\phi_k-\phi_n)\Big]\\
-\;& \frac{\Lambda}{N^3}\Big[\sum_{k=1}^{N}\sum_{j=1}^{N}\left(\frac{\cos(\phi_k-\phi_j)}{2}\cos(\omega\Delta+\phi_n) + \frac{\cos(\omega\Delta-\phi_n+\phi_j+\phi_k)}{4}\right)\Big]\\
+\;& \frac{\Lambda}{4N^2}\Big[\sum_{k=1}^{N}\left(\cos(\omega\Delta+\phi_k) + \frac{1}{2}\cos(\omega\Delta+2\phi_n-\phi_k)\right)\Big] - \frac{\Lambda}{8N}\cos(\omega\Delta+\phi_n)\Bigg]
\end{aligned} \tag{4.38}$$

- Equation of $\sin(\omega t)$:

$$\begin{aligned}
&-\omega\cos(\phi_n) + \mu\sin(\phi_n) + \frac{\Lambda}{N}\sin(\omega\Delta+\phi_n) = \frac{\Lambda}{N^2}\sum_{k=1}^{N}\sin(\omega\Delta+\phi_k)\\
+\;& a^2\Bigg[\frac{\Lambda}{8N^2}\sum_{k=1}^{N}\sin(\omega\Delta+\phi_k) - \frac{\Lambda}{N^3}\Big[\frac{N}{2}\sum_{k=1}^{N}\sin(\omega\Delta+\phi_k) + \frac{1}{4}\sum_{k=1}^{N}\sum_{j=1}^{N}\sin(\omega\Delta+2\phi_k+\phi_j)\Big]\\
+\;& \frac{\Lambda}{N^4}\Big[\sum_{i=1}^{N}\sum_{k=1}^{N}\sum_{j=1}^{N}\left(\frac{\cos(\phi_j-\phi_k)}{2}\sin(\omega\Delta+\phi_i) + \frac{\sin(\omega\Delta+\phi_j+\phi_k-\phi_i)}{4}\right)\Big]\\
+\;& \frac{\Lambda}{4N^2}\Big[N\sin(\omega\Delta+\phi_n) + \sum_{k=1}^{N}\sin(\omega\Delta+2\phi_k-\phi_n)\Big]\\
-\;& \frac{\Lambda}{N^3}\Big[\sum_{k=1}^{N}\sum_{j=1}^{N}\left(\frac{\cos(\phi_k-\phi_j)}{2}\sin(\omega\Delta+\phi_n) + \frac{\sin(\omega\Delta-\phi_n+\phi_j+\phi_k)}{4}\right)\Big]\\
+\;& \frac{\Lambda}{4N^2}\Big[\sum_{k=1}^{N}\left(\sin(\omega\Delta+\phi_k) + \frac{1}{2}\sin(\omega\Delta+2\phi_n-\phi_k)\right)\Big] - \frac{\Lambda}{8N}\sin(\omega\Delta+\phi_n)\Bigg]
\end{aligned} \tag{4.39}$$

Perturbing the time delay Δ and the frequency ω around the corresponding critical values as follows

$$\Delta = \Delta_c + \delta \qquad \text{and} \qquad \omega = \omega_c + \omega_1 \tag{4.40}$$

where δ and ω_1 are the deviations from the critical time delay Δ_c and the critical frequency ω_c, respectively. Then, applying a Taylor series around Δ_c and ω_c up to the second order, Eqs.(4.38) and (4.39) can be written as

$$\omega_1 \sin(\phi_n) - \frac{\Lambda}{N}(\omega_c\delta + \Delta_c\omega_1)\sin(\omega_c\Delta_c + \phi_n) = a^2\left(\Gamma_1 + \Gamma_2(\omega_c\delta + \Delta_c\omega_1)\right) \tag{4.41}$$

$$\omega_1 \cos(\phi_n) - \frac{\Lambda}{N}(\omega_c\delta + \Delta_c\omega_1)\cos(\omega_c\Delta_c + \phi_n) = a^2\left(\Gamma_2 - \Gamma_1(\omega_c\delta + \Delta_c\omega_1)\right). \tag{4.42}$$

Equations (4.41) and (4.42) lead to the following frequency deviation ω_1 and amplitude a

$$\omega_1 = \frac{-(\alpha_2 + 2\alpha_1\omega_c)\delta - \alpha_3 \pm \sqrt{(\alpha_2\delta + \alpha_3)^2 - 4\delta\alpha_1\alpha_4}}{2\alpha_1\Delta_c} \tag{4.43}$$

$$a = \sqrt{\frac{\omega_1 \sin(\phi_i) - \frac{\Lambda}{N}(\omega_c\delta + \Delta_c\omega_1)\sin(\omega_c\Delta_c + \phi_i)}{\Gamma_1 + \Gamma_2(\omega_c\delta + \Delta_c\omega_1)}}. \tag{4.44}$$

A positive amplitude a is the only physically acceptable solution. The parameters of Eqs.(4.41), (4.42), (4.43) and (4.44) are given in Appendix A.
Figure 4.2 shows the lengths amplitudes of various queues numbers given by the Harmonic balance method (4.44) and the numerically computed amplitudes of Eq.(2.7). Figure 4.2 shows that the derived amplitude (4.44) is accurate, as expected, only in the vicinity of the critical time delays where the fundamental frequency is dominant.

Figure 4.3 shows the queue length oscillation frequencies of various queues numbers given by the Harmonic balance method and the numerically computed frequencies of Eq.(2.7). Figure 4.3 shows that the accuracy domain of the analytically derived frequencies improves by increasing the number of queues. This result is due to the effect of nonlinearities that is decreasing with increasing the number of queues.

5 Multiple Scales Method

. The objective of this section is to obtain an accurate analytical expression of the limit cycles better than the one given by the HBM. Hence, we will use the multiple scales method (MSM) Nayfeh [21], Nayfeh et al. [22] adapted to delay differential equations Rand [30]. The MSM is a perturbation method that is characterized by the introduction of independent scales of time and consequently the transformation of DDEs to a set of linear delayed partial differential equations.
In comparison to the HB method, the MSM provides an analytical approximation of periodic solutions, including higher harmonics, and their stabilities. It also makes it possible to study the transient phase, which allows us to understand how the amplitude grows over time or shrinks over time depending on whether a Hopf bifurcation has occurred.

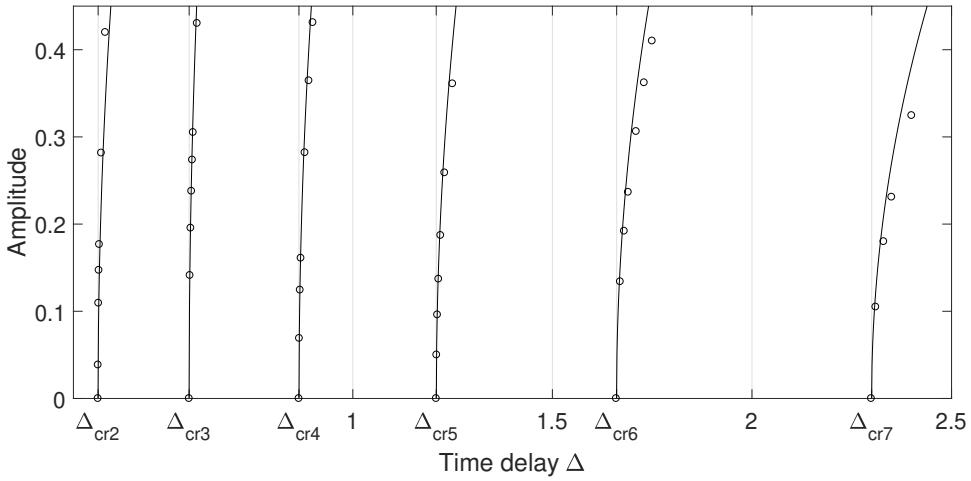

Figure 4.2: Amplitude versus time delay for various number of queues. Continuous lines show the HBM amplitude given by Eq.(4.44) and circles correspond to amplitudes computed by numerical integration of Eqs. (2.7)

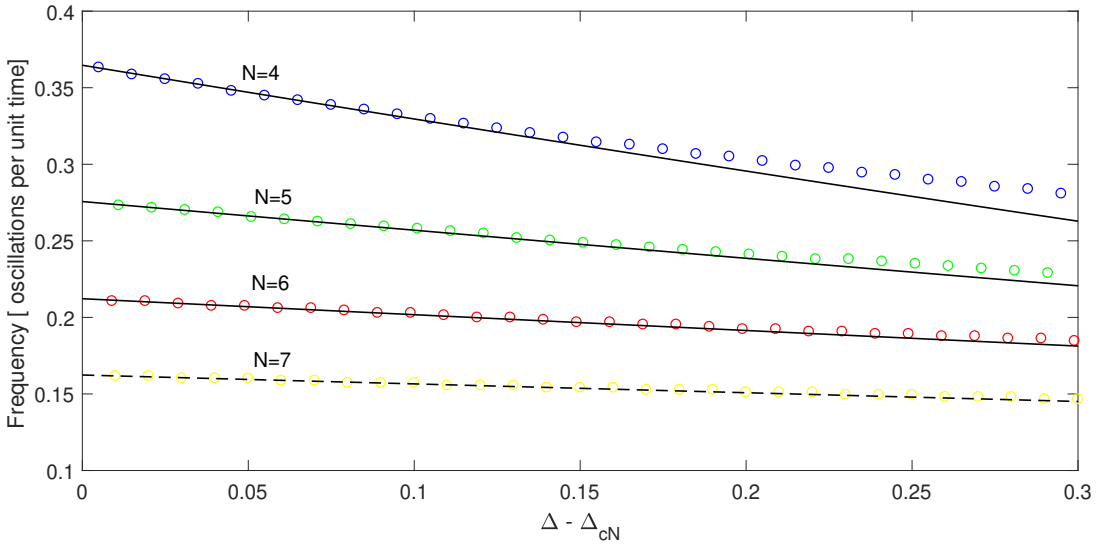

Figure 4.3: Frequency versus the deviation $\Delta - \Delta_{c,N}$ of the time delay from its critical values for various number of queues. Continuous lines show the HBM frequencies and circles correspond to frequencies computed by numerical integration of Eqs. (2.7)

5.1 Case of N queues

A small positive parameter ε is introduced into Eq. (3.18) in order to scale nonlinearities and to trigger the perturbation process. Hence, the queue length differences $D_n(t)$ are written as follows

$$D_n(t) = \varepsilon X_n(t), \quad \text{with } n = 1, ..., N \neq J. \tag{5.45}$$

Hence, using the transformation (5.45), Eq. (3.18) becomes

$$\begin{aligned}
\dot{X}_n + \mu X_n + \frac{\Lambda}{N} X_{n\Delta} &= \Lambda \Bigg[\varepsilon \Bigg[\left(\frac{2-N}{2N^2} \right) X_{n\Delta}^2 + \frac{1}{N^2} X_{n\Delta} \sum_{\substack{k=1 \\ k \neq \{n,J\}}}^{N} X_{k\Delta} \Bigg] \\
&+ \varepsilon^2 \Bigg[\left(\frac{-N^2 + 6N - 6}{6N^3} \right) X_{n\Delta}^3 + \left(\frac{N-4}{2N^3} \right) X_{n\Delta}^2 \sum_{\substack{k=1 \\ k \neq \{n,J\}}}^{N} X_{k\Delta} \\
&+ \frac{1}{2N^2} X_{n\Delta} \Bigg(\sum_{\substack{k=1 \\ k \neq \{n,J\}}}^{N} X_{k\Delta}^2 - \frac{2}{N} \left(\sum_{\substack{k=1 \\ k \neq \{n,J\}}}^{N} X_{k\Delta} \right)^2 \Bigg) \Bigg] \Bigg].
\end{aligned} \tag{5.46}$$

Moreover, the time delay Δ is expanded in terms of ε, beyond the critical delay Δ_c that causes a Hopf bifurcation, as follows $\Delta = \Delta_c + \delta = \Delta_c + \varepsilon^2 \tilde{\delta}$.
The presence of quadratic nonlinearities in the model necessitates the use of three time scales i.e., the time $t = t(t_0, t_1, t_2)$, where the different independent time scales are $t_n = \varepsilon^n t$, with $n \in \mathbb{N}$. Using the chain rule, the time derivative is expressed as follows

$$\frac{d()}{dt} = \frac{\partial()}{\partial t_0} + \varepsilon \frac{\partial()}{\partial t_1} + \varepsilon^2 \frac{\partial()}{\partial t_2} + \mathcal{O}(\varepsilon^3). \tag{5.47}$$

Solutions and their delayed versions are expressed in terms of the small parameter ε as follows

$$X_n(t) = X_{n,0}(t_0, t_1, t_2) + \varepsilon X_{n,1}(t_0, t_1, t_2) + \varepsilon^2 X_{n,2}(t_0, t_1, t_2) + \mathcal{O}(\varepsilon^3) \tag{5.48}$$

$$\begin{aligned}
X_n(t - \Delta) &= X_n(t_0 - \Delta, t_1 - \varepsilon\Delta, t_2 - \varepsilon^2\Delta, ...) \\
&= X_{n,0}(t_0 - \Delta_c, t_1, t_2) + \varepsilon \Bigg(- \Delta_c \frac{\partial X_{n,0}(t_0 - \Delta_c, t_1, t_2)}{\partial t_1} + X_{n,1}(t_0 - \Delta_c, t_1, t_2) \Bigg) \\
&+ \varepsilon^2 \Bigg(- \tilde{\delta} \frac{\partial X_{n,0}(t_0 - \Delta, t_1, t_2)}{\partial (t_0 - \Delta_c)} - \frac{\Delta_c^2}{2} \frac{\partial^2 X_{n,0}(t_0 - \Delta_c, t_1, t_2)}{\partial t_1^2} - \Delta_c \frac{\partial X_{n,0}(t_0 - \Delta_c, t_1, t_2)}{\partial t_2} \\
&- \Delta_c \frac{\partial X_{n,1}(t_0 - \Delta_c, t_1, t_2)}{\partial t_1} + X_{n,2}(t_0 - \Delta_c, t_1, t_2) \Bigg) + \mathcal{O}(\varepsilon^3).
\end{aligned} \tag{5.49}$$

Inserting Eqs. (5.47), (5.48) and (5.49) into Eq. (5.46), and equating coefficients of like powers of ε, we get the following linear partial differential equations at different orders of ε

- Order $\mathcal{O}(\varepsilon^0)$

$$\frac{\partial X_{n,0}}{\partial t_0} + \mu X_{n,0} + \frac{\lambda}{N} X_{n,0}(t_0 - \Delta_c) = 0. \tag{5.50}$$

The solutions of Eqs.(5.50) are given by

$$X_{n,0}(t) \;=\; A_n(t_1, t_2)\exp(i\omega_c t_0) + \bar{A}_n(t_1, t_2)\exp(-i\omega_c t_0) \tag{5.51}$$

where the frequency ω_c and the critical delay Δ_c at the Hopf bifurcation are

$$\omega_c = \sqrt{\frac{\Lambda^2}{N^2} - \mu^2} \quad ; \quad \Delta_c = \frac{-1}{\sqrt{\frac{\Lambda^2}{N^2} - \mu^2}} \arctan\left(\frac{1}{\mu}\sqrt{\frac{\Lambda^2}{N^2} - \mu^2}\right). \tag{5.52}$$

The complex amplitudes A_n and their conjugates $\bar{A}_n$ depend on the two slow time scales t_1 and t_2. They are determined by eliminating the secular terms at order $\mathcal{O}(\varepsilon^2)$.

- Order $\mathcal{O}(\varepsilon^1)$

$$\begin{aligned}\frac{\partial X_{n,1}}{\partial t_0} + \mu X_{n,1} + \frac{\Lambda}{N} X_{n,1}(t_0 - \Delta_c) \;&=\; -\frac{\partial X_{n,0}}{\partial t_1} + \frac{\Lambda\Delta_c}{N}\frac{\partial X_{n,0}(t_0 - \Delta_c)}{\partial t_1} \\ &+\; \frac{\Lambda(2-N)}{2N^2} X_{n,0}^2(t_0 - \Delta_c) \\ &+\; \frac{\Lambda}{N^2} X_{n,0}(t_0 - \Delta_c) \sum_{\substack{k=1 \\ k\neq\{i,J\}}}^{N} X_{k,0}(t - \Delta_c).\end{aligned} \tag{5.53}$$

The elimination of secular terms conditions are given by

$$\frac{\partial A_n(t_1, t_2)}{\partial t_1}\left(-1 + \frac{\Lambda\Delta_c}{N}\exp(-i\omega_c\Delta_c)\right) = 0 \Rightarrow \frac{\partial A_n(t_1, t_2)}{\partial t_1} = 0. \tag{5.54}$$

The particular solution of Eqs.(5.53) is given by

$$\begin{aligned}X_{n,1}(t) \;&=\; H_0\Big[(2-N)A_n\bar{A}_n + A_n \sum_{\substack{k=1 \\ k\neq\{n,J\}}}^{N} \bar{A}_k + \bar{A}_n \sum_{\substack{k=1 \\ k\neq\{n,J\}}}^{N} A_k\Big] \\ &+\; H\Big[(2-N)A_n^2 + 2A_n \sum_{\substack{k=1 \\ k\neq\{n,J\}}}^{N} A_k\Big]e^{i2\omega_c t_0} + \bar{H}\Big[(2-N)\bar{A}_n^2 + 2\bar{A}_n \sum_{\substack{k=1 \\ k\neq\{n,J\}}}^{N} \bar{A}_k\Big]e^{-i2\omega_c t_0}\end{aligned} \tag{5.55}$$

where

$$H_0 = \frac{\Lambda}{N\Lambda + N^2\mu} \quad ; \quad H = \frac{\Lambda}{2N}\left(\frac{e^{-i2\omega_c\Delta_c}}{i2\omega_c N + \Lambda e^{-i2\omega_c\Delta_c} + N\mu}\right) = H_r + iH_i \tag{5.56}$$

where H_r and H_i are the real and imaginary parts of H, respectively. They are given by

$$H_r \;=\; \left(\frac{\Lambda}{2N}\right)\frac{N\mu\cos(2\omega_c\Delta_c) - 2N\omega_c\sin(2\omega_c\Delta_c) + \Lambda}{N^2\mu^2 + 4N^2\omega_c^2 + \Lambda^2 + 2N\mu\Lambda\cos(2\omega_c\Delta_c) - 4N\Lambda\omega_c\sin(2\omega_c\Delta_c)} \tag{5.57}$$

$$H_i \;=\; \left(\frac{-\Lambda}{2}\right)\frac{\mu\sin(2\omega_c\Delta_c) + 2\omega_c\cos(2\omega_c\Delta_c)}{N^2\mu^2 + 4N^2\omega_c^2 + \Lambda^2 + 2N\mu\Lambda\cos(2\omega_c\Delta_c) - 4N\Lambda\omega_c\sin(2\omega_c\Delta_c)} \tag{5.58}$$

- Order $\mathcal{O}(\varepsilon^2)$

$$
\begin{aligned}
\frac{\partial X_{n,2}}{\partial t_0} + \mu X_{n,2} + \frac{\Lambda}{N} X_{n,2}(t_0 - \Delta_c) &= -\frac{\partial X_{n,0}}{\partial t_2} - \frac{\partial X_{n,1}}{\partial t_1} \\
&+ \frac{\Lambda}{N}\left[\tilde{\delta}\frac{\partial X_{n,0}(t-\Delta_c)}{\partial(t_0-\Delta)} + \frac{\Delta_c^2}{2}\frac{\partial^2 X_{n,0}(t_0-\Delta_c)}{\partial t_1^2}\right. \\
&+ \left.\Delta_c\frac{\partial X_{n,0}(t_0-\Delta)}{\partial t_2} + \Delta_c\frac{\partial X_{n,1}(t_0-\Delta_c)}{\partial t_1}\right] \\
&+ \frac{\Lambda(2-N)}{N^2} X_{n,0}(t_0-\Delta_c)\left(X_{n,1}(t_0-\Delta_c) - \Delta_c\frac{\partial X_{n,0}(t_0-\Delta_c)}{\partial t_1}\right) \\
&+ \frac{\Lambda}{N^2} X_{n,0}(t_0-\Delta_c)\sum_{\substack{k=1\\k\neq\{n,J\}}}^{N}\left(X_{k,1}(t_0-\Delta) - \Delta_c\frac{\partial X_{k,0}(t_0-\Delta_c)}{\partial t_1}\right) \\
&+ \frac{\Lambda}{N^2}\left(X_{n,1}(t_0-\Delta) - \Delta_c\frac{\partial X_{n,0}(t_0-\Delta_c)}{\partial t_1}\right)\sum_{\substack{k=1\\k\neq\{n,J\}}}^{N} X_{k,0}(t_0-\Delta_c) \\
&+ \Lambda\left(\frac{-N^2+6N-6}{6N^3}\right) X_{n,0}^3(t_0-\Delta_c) \\
&+ \Lambda\left(\frac{N-4}{2N^3}\right) X_{n,0}^2(t_0-\Delta_c)\sum_{\substack{k=1\\k\neq\{n,J\}}}^{N} X_{k,0}(t_0-\Delta) \\
&+ \frac{\Lambda}{2N^2} X_{n,0}(t-\Delta_c)\Bigg(\sum_{\substack{k=1\\k\neq\{n,J\}}}^{N} X_{k,0}^2(t_0-\Delta_c) \\
&- \frac{2}{N}\left(\sum_{\substack{k=1\\k\neq\{n,J\}}}^{N} X_{k,0}(t_0-\Delta_c)\right)^2\Bigg). \qquad (5.59)
\end{aligned}
$$

The elimination of secular terms condition is given by

$$\begin{aligned}
\frac{\partial A_n}{\partial t_2} &= \left(\frac{e^{i\omega_c\Delta_c}}{\lambda}-\frac{\Delta_c}{N}\right)^{-1}\Bigg[i\frac{\tilde{\delta}}{N}\omega_c A_n + R_1 A_n^2\bar{A}_n + R_2 A_n^2\left(\sum_{\substack{k=1\\k\neq\{n,J\}}}^{N}\bar{A}_k\right)\\
&+ \bar{A}_n\Bigg[R_3\left(\sum_{\substack{k=1\\k\neq\{n,J\}}}^{N}A_k^2\right)+R_4\Bigg(\sum_{\substack{k=1\\k\neq\{n,J\}}}^{N}A_k\Bigg)^2\Bigg]+R_5A_n\bar{A}_n\left(\sum_{\substack{k=1\\k\neq\{n,J\}}}^{N}A_k\right)\\
&+ A_n\Bigg[\sum_{\substack{k=1\\k\neq\{n,J\}}}^{N}\left(R_6A_k\bar{A}_k+R_7A_k\sum_{\substack{j=1\\j\neq\{k,J,n\}}}^{N}\bar{A}_j+R_7\bar{A}_k\sum_{\substack{j=1\\j\neq\{k,J,n\}}}^{N}A_j\right)\Bigg]\\
&+ R_8A_n\left(\sum_{\substack{k=1\\k\neq\{n,J\}}}^{N}A_k\right)\left(\sum_{\substack{k=1\\k\neq\{n,J\}}}^{N}\bar{A}_k\right)+R_9\bar{A}_n\Bigg(\sum_{\substack{k=1\\k\neq\{n,J\}}}^{N}A_k\sum_{\substack{j=1\\j\neq\{k,J,n\}}}^{N}A_j\Bigg)\Bigg] \quad (5.60)
\end{aligned}$$

where the parameters $R_j(j=1,..,9)$ are given in Appendix B.
Writing the complex amplitude A_n in polar form as follows

$$A_n(t_1,t_2)=\frac{a_n(t_1,t_2)}{2}e^{i\theta_n(t_1,t_2)},\qquad \text{where } n=1,...,N\neq J. \quad (5.61)$$

Inserting the polar form (5.61) into the solvability condition (5.60) and separating real and imaginary parts, we obtain the following modulations equations of the amplitude $a_n(t)$ and the phase $\theta_n(t)$

$$\begin{aligned}
\dot{a}_n &= \Bigg[G_0\delta a_n+G_1a_n^3+a_n^2\Bigg[\sum_{\substack{k=1\\k\neq\{n,J\}}}^{N}a_k\Big(G_2\cos(\Psi_k)+G_3\sin(\Psi_k)\Big)\Bigg]\\
&+ a_n\Bigg[\sum_{\substack{k=1\\k\neq\{n,J\}}}^{N}a_k^2\Big(G_4+G_5\cos(2\Psi_k)+G_6\sin(2\Psi_k)\Big)\\
&+ \sum_{\substack{k=1\\k\neq\{n,J\}}}^{N}a_k\Bigg(\sum_{\substack{j=k+1\\j\neq\{n,J\}}}^{N}a_j\left(G_7\cos(\Psi_k+\Psi_j)+G_8\sin(\Psi_k+\Psi_j)+G_9\cos(\Psi_k-\Psi_j)\right)\\
&+ \sum_{\substack{j=1\\j\neq\{k,J,n\}}}^{N}a_j\left(G_{10}\cos(\Psi_k+\Psi_j)-G_{11}\sin(\Psi_k+\Psi_j)\right)\Bigg)\Bigg]\Bigg] \quad (5.62)
\end{aligned}$$

$$
\begin{aligned}
\dot{\theta}_n &= \Bigg[C_0\delta + C_1 a_n^2 + a_n\Bigg[\sum_{\substack{k=1\\k\neq\{n,J\}}}^{N} a_k\left(C_2\cos(\Psi_k) + C_3\sin(\Psi_k)\right)\Bigg] \\
&+ \Bigg[\sum_{\substack{k=1\\k\neq\{n,J\}}}^{N} a_k^2\Big(C_4 + C_5\cos(2\Psi_k) - C_6\sin(2\Psi_k)\Big) \\
&+ \sum_{\substack{k=1\\k\neq\{n,J\}}}^{N} a_k\Bigg(\sum_{\substack{j=k+1\\j\neq\{n,J\}}}^{N} a_j\left(-C_7\sin(\Psi_k+\Psi_j) + C_8\cos(\Psi_k+\Psi_j) + C_9\cos(\Psi_k-\Psi_j)\right) \\
&+ \sum_{\substack{j=1\\j\neq\{k,J,n\}}}^{N} a_j\left(G_{11}\cos(\Psi_k+\Psi_j) - G_{10}\sin(\Psi_k+\Psi_j)\right)\Bigg)\Bigg]\Bigg] \qquad (5.63)
\end{aligned}
$$

where $\Psi_k = \theta_n - \theta_k$. The parameters $G_j(j = 0, .., 11)$ and $C_j(j = 0, .., 9)$ are given in Appendix B.
A sufficient condition for a periodic solution of Eq.(5.45) is to have a nontrivial constant amplitude a_n^*, zero of Eq.(5.62), and a constant $\dot{\theta}_n$, given in Eq.(5.63). Up to the second order, the n^{th} queue length difference $D_n(t)$, periodic solution of Eq. (3.18) is given by

$$
\begin{aligned}
D_n(t) &= a_n^*\cos(\Omega t + \theta_{n0}) + H_0\left[\frac{2-N}{4}a_n^{*2} + \frac{a_n^*}{2}\sum_{\substack{k=1\\k\neq\{n,J\}}}^{N} a_k^*\cos(\theta_{n0}-\theta_{k0})\right] \\
&+ H_{nr}\left[\frac{2-N}{2}a_n^{*2}\cos(2\Omega t + 2\theta_{n0}) + a_n^*\sum_{\substack{k=1\\k\neq\{n,J\}}}^{N} a_k^*\cos(2\Omega t + \theta_{k0} + \theta_{n0})\right] \\
&- H_{ni}\left[\frac{2-N}{2}a_n^{*2}\sin(2\Omega t + 2\theta_{n0}) + a_n^*\sum_{\substack{k=1\\k\neq\{n,J\}}}^{N} a_k^*\sin(2\Omega t + \theta_{k0} + \theta_{n0})\right] \qquad (5.64)
\end{aligned}
$$

where $\theta_{m0} = \theta_m(0), \forall m = 1, ..., N$.

5.2 Particular cases of two and three queues

In this subsection, the cases of two and three queues are investigated since they correspond to the case where nonlinearities and couplings are the strongest.

5.2.1 Case of two queues

Choosing the first queue as a reference $J = 1$, the amplitude and phase modulation equations (5.62) and (5.63) of the queues lengths difference $D_2(t) = Q_1(t) - Q_2(t)$ are given by

$$
\dot{a}_2 = G_0\delta a_2 + G_1 a_2^3 \quad ; \quad \dot{\theta}_2 = C_0\delta + C_1 a_2^2 \qquad (5.65)
$$

where

$$G_0 = -\beta_2 \frac{\omega_{c2}}{2} \quad ; \quad G_1 = \frac{\beta_1}{32} \quad ; \quad C_0 = \beta_1 \frac{\omega_{c2}}{2} \quad ; \quad C_1 = \frac{\beta_2}{32} \tag{5.66}$$

The amplitude of the periodic solution, corresponding to $\dot{a}_2 = 0$, is given by

$$a_2^* = \sqrt{-\frac{G_0 \delta}{G_1}} = 4\sqrt{\frac{\beta_2 \omega_{c2}}{\beta_1}\delta}. \tag{5.67}$$

The phase $\theta_2(t)$ is given by

$$\theta_2(t) = \left(C_0\delta + C_1 a_2^{*2}\right) t + \theta_{20}. \tag{5.68}$$

Consequently, the fundamental frequency Ω of the periodic solution is given by

$$\Omega = \omega_{c2} + C_0\delta + C_1 a_2^{*2} = \omega_{c2}\left(1 + \left(\frac{\beta_1^2 + \beta_2^2}{2\beta_1}\right)\delta\right) \tag{5.69}$$

The solution of the queue length difference (5.64) becomes in the case of two queues $D_2(t)$ up to the second order

$$D_2(t) = a_2^* \cos(\Omega t + \theta_{20}) + \mathcal{O}(\varepsilon^2). \tag{5.70}$$

The length queues equation (3.20) leads to the following expressions

$$Q_1(t) = \frac{\Lambda}{2\mu} + \frac{1}{2} D_2(t) \tag{5.71}$$

$$Q_2(t) = \frac{\Lambda}{2\mu} - \frac{1}{2} D_2(t) = Q_1(t + \pi). \tag{5.72}$$

These two solutions are out of phase.

5.2.2 Case of three queues

Choosing the first line as a reference $J = 1$, the length differences are defined as $D_2(t) = Q_1(t) - Q_2(t)$ and $D_3(t) = Q_1(t) - Q_3(t)$. They are governed by the following two nonlinear delay differential equations

$$\dot{D}_2 = \frac{\Lambda}{54}\left[-18D_{2\Delta} - 3D_{2\Delta}^2 + D_{2\Delta}^3 + 6D_{2\Delta}D_{3\Delta} - D_{2\Delta}^2 D_{3\Delta} + D_{2\Delta}D_{3\Delta}^2 \right] - \mu D_2 \tag{5.73}$$

$$\dot{D}_3 = \frac{\Lambda}{54}\left[-18D_{3\Delta} - 3D_{3\Delta}^2 + D_{3\Delta}^3 + 6D_{3\Delta}D_{2\Delta} - D_{3\Delta}^2 D_{2\Delta} + D_{3\Delta}D_{2\Delta}^2 \right] - \mu D_3 \tag{5.74}$$

The amplitude and phase modulation equations (5.62) and (5.63) become in the case of three queues as follows

$$\begin{aligned}
\dot{a}_2 &= S_1\delta a_2 + S_2 a_2^3 + S_3 a_2 a_3^2 + (-S_2\cos(\Psi) + S_4\sin(\Psi))\, a_2^2 a_3 \qquad (5.75)\\
&+ (S_5\cos(2\Psi) - S_4\sin(2\Psi))\, a_2 a_3^2\\
\dot{a}_3 &= S_1\delta a_3 + S_2 a_3^3 + S_3 a_3 a_2^2 - (S_2\cos(\Psi) + S_4\sin(\Psi))\, a_2 a_3^2 \qquad (5.76)\\
&+ (S_5\cos(2\Psi) + S_4\sin(2\Psi))\, a_2^2 a_3\\
\dot{\Psi} &= (M_2 - M_3 + S_4\cos(2\Psi))\,(a_2^2 - a_3^2) + 2S_5 a_2 a_3\sin(\Psi) - S_5(a_2^2 + a_3^2)\sin(2\Psi)\\
&= -S_4\,(1 - \cos(2\Psi))\,(a_2^2 - a_3^2) + 2S_5 a_2 a_3\sin(\Psi) - S_5(a_2^2 + a_3^2)\sin(2\Psi). \qquad (5.77)
\end{aligned}$$

where $\Psi = \theta_2 - \theta_3$ is the difference of phases. All the newly introduced parameters are given in Appendix C.

The vector field of the slow flow equations, (5.75), (5.76) and (5.77), is invariant with respect to the permutation $\mathcal{P}(a_2, a_3) = (a_3, a_2)$ and the symmetry $\mathcal{T}(\Psi) = -\Psi$. Moreover, a sufficient condition to have periodic solutions of the original equations (5.73) and (5.74) is to use equilibria of Eqs. (5.75), (5.76) and (5.77). The stability of these solutions can be investigated by computing the eigenvalues of the Jacobian of the slow flow. Equations (5.75), (5.76) and (5.77) have a family of equilibria corresponding to the case of equal amplitudes i.e., $a_2 = a_3 = a_3^*$. These equilibria are given, in the case of non-negative Ψ_s, by

$$\begin{aligned}
\mathcal{P}_1 &= \left(a_3^* = \sqrt{-\frac{\delta S_1}{S_3 + S_5}}, a_3^* = \sqrt{-\frac{\delta S_1}{S_3 + S_5}}, \Psi_s = 0\right) \qquad (5.78)\\
\mathcal{P}_2 &= \left(a_3^* = \sqrt{-\frac{\delta S_1}{2S_2 + S_3 + S_5}}, a_3^* = \sqrt{-\frac{\delta S_1}{2S_2 + S_3 + S_5}}, \Psi_s = \pi\right) \qquad (5.79)\\
\mathcal{P}_3 &= \left(a_3^* = \sqrt{-\frac{2\delta S_1}{S_2 + 2S_3 - S_5}}, a_3^* = \sqrt{-\frac{2\delta S_1}{S_2 + 2S_3 - S_5}}, \Psi_s = \frac{\pi}{3}\right). \qquad (5.80)
\end{aligned}$$

In our case, only the fixed point $\mathcal{P}_3$ is stable, see Appendix D.

In Appendix E, it is proven that the fundamental frequency Ω of the limit cycle is given by

$$\Omega = \omega_c + \delta\left(M_1 - S_1\frac{M_2 + 2M_3 + S_4}{S_2 + 2S_3 - S_5}\right). \qquad (5.81)$$

The frequency Ω is changing linearily with respect to δ while the amplitude a_3^*, given in Eq.(5.80), is increasing proportional to $\sqrt{\delta}$. The approximation of the limit cycles up to the second order, of Eqs. (5.73) and (5.74), are given by

$$\begin{aligned}
D_2(t) &= a_3^*\cos(\Omega t + \theta_{20}) + a_3^{*2}\left[H_r\left(-\frac{1}{2}\cos(2\Omega t + 2\theta_{20}) + \cos(2\Omega t + \theta_{20} + \theta_{30})\right)\right.\\
&+ \left. H_i\left(\frac{1}{2}\sin(2\Omega t + 2\theta_{20}) - \sin(2\Omega t + \theta_{20} + \theta_{30})\right)\right] + \mathcal{O}(\varepsilon^2) \qquad (5.82)\\
D_3(t) &= a_3^*\cos(\Omega t + \theta_{30}) + a_3^{*2}\left[H_r\left(-\frac{1}{2}\cos(2\Omega t + 2\theta_{30}) + \cos(2\Omega t + \theta_{20} + \theta_{30})\right)\right.\\
&+ \left. H_i\left(\frac{1}{2}\sin(2\Omega t + 2\theta_{30}) - \sin(2\Omega t + \theta_{20} + \theta_{30})\right)\right] + \mathcal{O}(\varepsilon^2) \qquad (5.83)
\end{aligned}$$

where $\theta_{20} = \theta_2(0)$ and $\theta_{30} = \theta_3(0)$ are the phases at initial time $t = 0$ of $D_2(t)$ and $D_3(t)$, respectively. They have to verify the constraint $\theta_{20} - \theta_{30} = \Psi_s = \pi/3$.
The lengths of the three queues are find using the following three relations

$$q_1(t) - q_2(t) = \frac{D_2(t)}{\gamma} \quad ; \quad q_1(t) - q_3(t) = \frac{D_3(t)}{\gamma} \quad ; \quad q_1(t) + q_2(t) + q_3(t) = \frac{\lambda}{\mu}. \quad (5.84)$$

Consequently, we get the following solutions

$$q_1(t) = \frac{\lambda}{3\mu} + \frac{1}{3\gamma}(D_2(t) + D_3(t)) \quad (5.85)$$

$$q_2(t) = \frac{\lambda}{3\mu} + \frac{1}{3\gamma}(D_3(t) - 2D_2(t)) \quad (5.86)$$

$$q_3(t) = \frac{\lambda}{3\mu} + \frac{1}{3\gamma}(D_2(t) - 2D_3(t)). \quad (5.87)$$

Up to the first order, using Eqs. (5.82) and (5.83), the lengths of the three queues, are given explicitely by

$$q_1(t) = \frac{\lambda}{3\mu} + \frac{a_3^*}{\gamma\sqrt{3}} \cos\left(\Omega t + \theta_{20} - \frac{\pi}{6}\right) + \mathcal{O}(\varepsilon) \quad (5.88)$$

$$q_2(t) = q_1\left(t - \frac{2\pi}{3\Omega}\right) = \frac{\lambda}{3\mu} + \frac{a_3^*}{\gamma\sqrt{3}} \cos\left(\Omega t + \theta_{20} - \frac{5\pi}{6}\right) + \mathcal{O}(\varepsilon) \quad (5.89)$$

$$q_3(t) = q_1\left(t + \frac{2\pi}{3\Omega}\right) = \frac{\lambda}{3\mu} + \frac{a_3^*}{\gamma\sqrt{3}} \cos\left(\Omega t + \theta_{20} + \frac{\pi}{2}\right) + \mathcal{O}(\varepsilon). \quad (5.90)$$

The lengths of each queue is oscillating around the equilibrium state with the same amplitude and the shift between two queues is $2\pi/3$.

5.3 Results

For all the numerical results $\lambda = 10$ and $\mu = 1$. In Fig. 5.1 are shown the graphs of the limit cycles in the plane $(D_2(t), D_3(t))$ for various values of the delay time Δ. This figure shows the good agreement between the numerical integration of the system of DDEs and the MSM analytical solutions (5.82) and (5.83).
In Fig. 5.2 are shown the limit cycles of the queues lengths in the space $(q_1(t), q_2(t), q_3(t)$, for $\Delta = 0.6, 0.7, 0.8$ and 0.9. This figure shows that increasing the time delay Δ increases the amplitude of the limit cycles. It proves the validity of analytical solutions obtained by the MSM up to the second order.

In Fig.5.3 are shown the numerical time histories of the three queues $q_1(t), q_2(t)$ and $q_3(t)$ for various initial starting function in the domain $[-\Delta, 0]$. Figure 5.3(a) shows that when the starting functions are different, the three queues have the same amplitude and frequency with a shift of $2\pi/3$ between each other. Figure 5.3(b) shows that if two queues are initially identical, they remain identical for all times with an amplitude equal one half the amplitude of the third queue. In this case, the three queues are behaving like two queues and they are out of phase. When the three queues are initially identical, Fig.5.3(c) shows that they

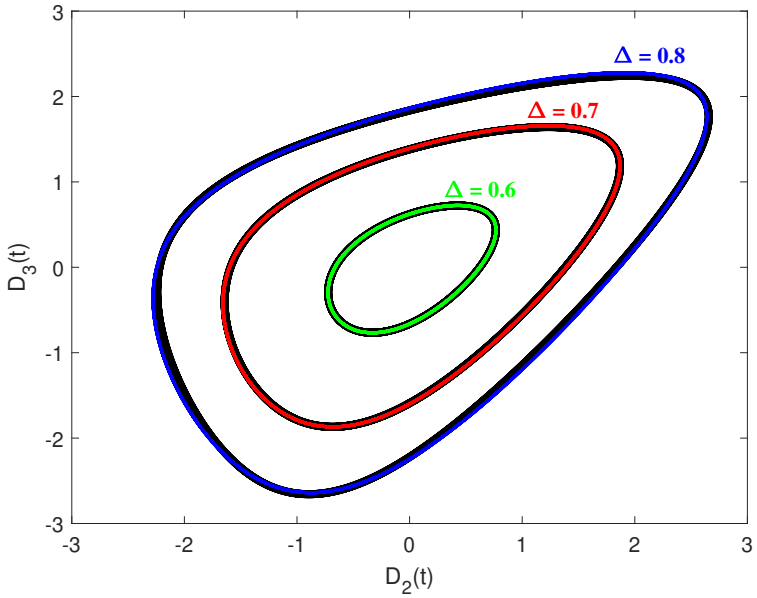

Figure 5.1: Limit cycles of Eqs. (5.73) and (5.74) for various time delays Δ. The analytical solutions (5.82) and (5.83) given by the MSM are shown in thick black lines and the numerical solutions are shown in blue, red and green.

are not oscillating and they converge to the static equilibrium $\lambda\gamma/3\mu$. Figures 5.3 show the sensitivity to the initial conditions and they illustrate our result stating that when $\Delta > \Delta_c$ the stable solution of the three queues problem is given in Fig.5.3(a).

In Fig. 5.4 are shown, in the case of two and three queues, the amplitudes of the periodic queues lengths, $q_n(t)$, versus the time delay Δ. We define the amplitude in the numerical simulations as the half of the difference between the maximum and the minimum of the steady state solution. The MSM amplitudes of the queues lengths oscillations $q_n(t)$ are $a_2^*/2$ for $N = 2$ and $a_3^*/(\gamma\sqrt{3})$ for $N = 3$. Figure 5.4 shows the good agreement between the MSM results and the numerical results in comparison to the HBM results.

6 Conclusion and Future Work

This paper answers important questions with regards to service systems using delayed information into their delay announcements. We consider the information passed to the customers about each of N queues is delayed by a constant Δ, which can be interpreted as the time of customers traveling to the selected queue. We prove explicit expressions for the critical delay, the amplitude, frequency, and the phases of each queue using the harmonic balance and the method of multiple scales. Unlike the harmonic balance method, the method of multiple scales provides the transient path of the amplitude dynamics.

There are many possible research topics for future work. The first would be to generalize the constant delay to a random delay. This would generalize the ddes to distributed delay equations. It is not only an open problem to understand how the critical delay depends

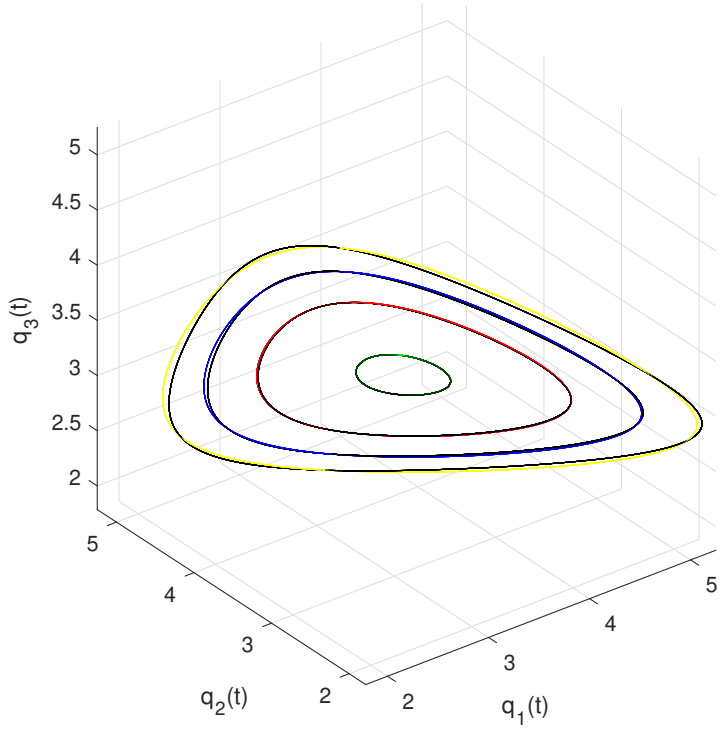

Figure 5.2: Limit cycles of queues lengths $q_1(t), q_2(t)$ and $q_3(t)$ for various time delays. The analytical solutions (5.85), (5.86) and (5.87) given by the MSM are shown in black lines and the numerical solutions are shown in green ($\Delta = 0.6$), red ($\Delta = 0.7$), blue ($\Delta = 0.8$) and yellow ($\Delta = 0.9$).

on the distribution of the random variable, but also how the amplitude and the frequency depend on it as well. A second generalization would be apply the delayed information to more complicated queueing models. We do not mean applying it to the Erlang-A as the infinite server case analysis can be easily applied to the Erlang-A model. One example would be models that are not symmetric and perhaps queues that are connected i.e. a Jackson network. We plan to pursue these extensions in future work.

Acknowledgements

This work was completed during the visit of Faouzi Lakrad to Cornell University. His visit was supported by a three month Fulbright fellowship. Jamol Pender gratefully acknowledges the support of National Science Foundation (NSF) for Jamol Pender's Career Award CMMI # 1751975.

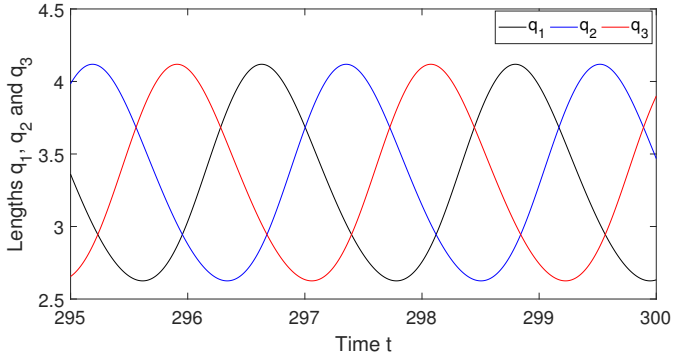

(a) $q_1(t) = 1, q_2(t) = 1.01, q_3(t) = 0.99$, for $t \in [-\Delta, 0]$

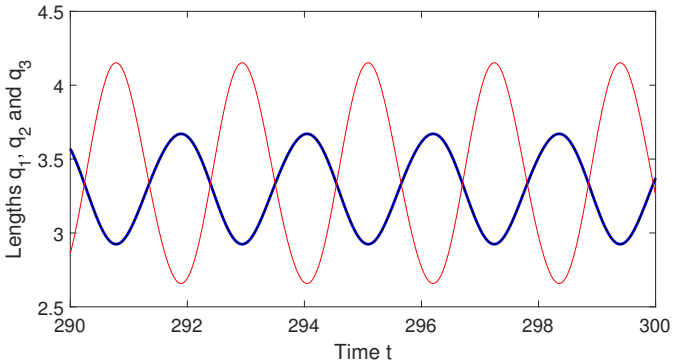

(b) $q_1(t) = q_2(t) = 1, q_3(t) = 0.99$, for $t \in [-\Delta, 0]$

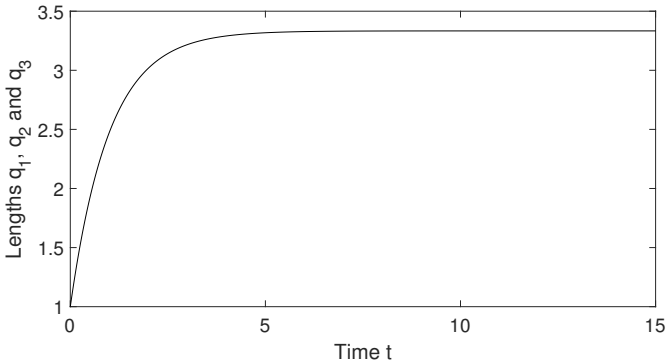

(c) $q_1(t) = q_2(t) = q_3(t) = 1$, for $t \in [-\Delta, 0]$

Figure 5.3: Time histories of queues lengths for $N = 3, \gamma = 1$ and $\Delta = 0.65$ and for various initial conditions

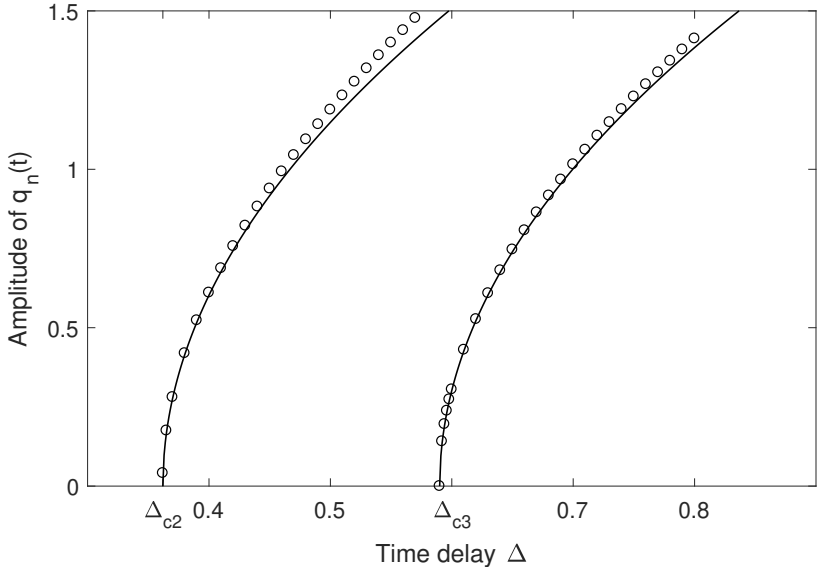

Figure 5.4: Amplitude of the periodic solution of the queues lengths versus the time delay Δ for two and three queues. Continuous line is obtained through the MSM and circles are obtained by numerical integrations

Appendix A: Parameters of the HBM

The parameters, obtained through the HBM, of Eqs.(4.41), (4.42), (4.43) and (4.44) are given by

$$\begin{aligned}
\Gamma_1 &= -\frac{\Lambda}{4N^3}\sum_{k=1}^{N}\sum_{j=1}^{N}\left(\cos(\omega_c\Delta_c+2\phi_k+\phi_j)\right) \\
&+ \frac{\Lambda}{N^4}\sum_{i=1}^{N}\sum_{k=1}^{N}\sum_{j=1}^{N}\left(\frac{\cos(\phi_j-\phi_k)}{2}\cos(\omega_c\Delta_c+\phi_i)+\frac{1}{4}\cos(\omega_c\Delta_c+\phi_j+\phi_k-\phi_i)\right) \\
&+ \frac{\Lambda}{4N^2}\Big[N\cos(\omega_c\Delta_c+\phi_n)+\sum_{k=1}^{N}\cos(\omega_c\Delta_c+2\phi_k-\phi_n)\Big] \\
&- \frac{\Lambda}{N^3}\Big[\sum_{k=1}^{N}\sum_{j=1}^{N}\left(\frac{\cos(\phi_j-\phi_k)}{2}\cos(\omega_c\Delta_c+\phi_n)+\frac{1}{4}\cos(\omega_c\Delta_c+\phi_j+\phi_k-\phi_n)\right)\Big] \\
&+ \frac{\Lambda}{8N^2}\sum_{k=1}^{N}\cos(\omega_c\Delta_c+2\phi_n-\phi_k)-\frac{\Lambda}{8N}\cos(\omega_c\Delta_c+\phi_n) \qquad (6.91)
\end{aligned}$$

$$
\begin{aligned}
\Gamma_2 &= \frac{\Lambda}{4N^3}\sum_{k=1}^{N}\sum_{j=1}^{N}(\sin(\omega_c\Delta_c+2\phi_k+\phi_j)) \\
&- \frac{\Lambda}{N^4}\sum_{i=1}^{N}\sum_{k=1}^{N}\sum_{j=1}^{N}\left(\frac{\cos(\phi_j-\phi_k)}{2}\sin(\omega_c\Delta_c+\phi_i)+\frac{1}{4}\sin(\omega_c\Delta_c+\phi_j+\phi_k-\phi_i)\right) \\
&- \frac{\Lambda}{4N^2}\Big[N\sin(\omega_c\Delta_c+\phi_n)+\sum_{k=1}^{N}\sin(\omega_c\Delta_c+2\phi_k-\phi_n)\Big] \\
&+ \frac{\Lambda}{N^3}\Big[\sum_{k=1}^{N}\sum_{j=1}^{N}\left(\frac{\cos(\phi_j-\phi_k)}{2}\sin(\omega_c\Delta_c+\phi_n)+\frac{1}{4}\sin(\omega_c\Delta_c+\phi_j+\phi_k-\phi_n)\right)\Big] \\
&- \frac{\Lambda}{8N^2}\sum_{k=1}^{N}\sin(\omega_c\Delta_c+2\phi_n-\phi_k)+\frac{\Lambda}{8N}\sin(\omega_c\Delta_c+\phi_n) \qquad (6.92)
\end{aligned}
$$

$$
\alpha_1 = -\Gamma_1\left(\frac{\sin(\phi_n)}{\Delta_c}-\frac{\Lambda}{N}\sin(\omega_c\Delta_c+\phi_n)\right)-\Gamma_2\left(\frac{\cos(\phi_n)}{\Delta_c}-\frac{\Lambda}{N}\cos(\omega_c\Delta_c+\phi_n)\right) \qquad (6.93)
$$

$$
\alpha_2 = \frac{\omega_c(\Gamma_1\sin(\phi_n)+\Gamma_2\cos(\phi_n))}{\Delta_c} \qquad (6.94)
$$

$$
\alpha_3 = -\Gamma_1\left(\frac{\cos(\phi_n)}{\Delta_c}-\frac{\Lambda}{N}\cos(\omega_c\Delta_c+\phi_n)\right)+\Gamma_2\left(\frac{\sin(\phi_n)}{\Delta_c}-\frac{\Lambda}{N}\sin(\omega_c\Delta_c+\phi_n)\right) \qquad (6.95)
$$

$$
\alpha_4 = -\frac{\omega_c}{\Delta_c}(\Gamma_2\sin(\phi_n)-\Gamma_1\cos(\phi_n)) \qquad (6.96)
$$

Appendix B: Parameters of the MSM

Parameters introduced in the secular term elimination equation (5.60)

$$R_1 = (H_0 + H)\frac{(2-N)^2}{N^2} + \left(\frac{-N^2+6N-6}{2N^3}\right) \tag{6.97}$$

$$R_2 = \frac{2-N}{N^2}H + \frac{3-N}{N^2}H_0 + \left(\frac{N-4}{2N^3}\right) \tag{6.98}$$

$$R_3 = \frac{1+2H(2-N)}{2N^2} \tag{6.99}$$

$$R_4 = \frac{H_0}{N^2} - \frac{1}{N^3} \tag{6.100}$$

$$R_5 = \frac{(5-2N)}{N^2}H_0 + \frac{2(3-N)}{N^2}H + \frac{N-4}{N^3} \tag{6.101}$$

$$R_6 = \frac{(3-N)H_0 + 2H}{N^2} \tag{6.102}$$

$$R_7 = \frac{H_0}{N^2} \tag{6.103}$$

$$R_8 = \frac{N-2}{N^3} \tag{6.104}$$

$$R_9 = \frac{2H}{N^2} \tag{6.105}$$

The real and the imaginary parts of each parameter R_j are denoted R_{jr} and R_{ji}, respectively.

$$\beta_1 + i\beta_2 = \left(\frac{e^{i\omega_c\Delta_c}}{\lambda} - \frac{\Delta_c}{N}\right)^{-1} \tag{6.106}$$

where

$$\beta_1 = \frac{N^2\Lambda\cos(\omega_c\Delta_c) - N\Lambda^2\Delta_c}{N^2 - 2N\Lambda\Delta_c\cos(\omega_c\Delta_c) + \Delta_c^2\Lambda^2} \tag{6.107}$$

$$\beta_2 = \frac{-N^2\Lambda\sin(\omega_c\Delta_c)}{N^2 - 2N\Lambda\Delta_c\cos(\omega_c\Delta_c) + \Delta_c^2\Lambda^2} \tag{6.108}$$

Parameters introduced in the amplitude and phase modulations equations (5.62) and (5.63) are given by

$$\begin{aligned}
G_0 &= -\beta_2\frac{\omega_c}{N}\ ;\ G_1=\frac{1}{4}(\beta_1 R_{1r}-\beta_2 R_{1i})\ ;\ G_2=\frac{\beta_1}{4}(R_{2r}+R_{5r})-\frac{\beta_2}{4}(R_{2i}+R_{5i})\\
G_3 &= (\beta_1 R_{5i}+\beta_2 R_{5r})/4-(\beta_1 R_{2i}+\beta_2 R_{2r})/4\ ;\ G_4=(\beta_1(R_{6r}+R_8)-\beta_2 R_{6i})/4\\
G_5 &= (\beta_1 R_{3r}-\beta_2 R_{3i})/4+\beta_1 R_4/4\ ;\ G_6=(\beta_1 R_{3i}+\beta_2 R_{3r})/4+\beta_2 R_4/4\\
G_7 &= \beta_1 R_4/2\ ;\ G_8=\beta_2 R_4/2\ ;\ G_9=(\beta_1 R_{8r}-\beta_2 R_{8i})/4+\beta_1 R_7/2\\
G_{10} &= (\beta_1 R_{9r}-\beta_2 R_{9i})/4\ ;\ G_{11}=(\beta_1 R_{9i}+\beta_2 R_{9r})/4\ ;\ C_0=\beta_1\frac{\omega_c}{N}\\
C_1 &= (\beta_2 R_{1r}+\beta_1 R_{1i})/4\ ;\ C_2=(\beta_1 R_{2i}+\beta_2 R_{2r})/4+(\beta_1 R_{5i}+\beta_2 R_{5r})/4\\
C_3 &= (\beta_1 R_{2r}-\beta_2 R_{2i})/4-(\beta_1 R_{5r}-\beta_2 R_{5i})/4\ ;\ C_4=(\beta_1 R_{6i}+\beta_2(R_{6r}+\beta_8))/4\\
C_5 &= (\beta_1 R_{3i}+\beta_2 R_{3r})/4+\beta_2 R_4/4\ ;\ C_6=(\beta_1 R_{3r}-\beta_2 R_{3i})/4+\beta_1 R_4/4\\
C_7 &= \beta_1 R_4/2\ ;\ C_8=\beta_2 R_4/2\ ;\ C_9=\beta_2 R_7/2+(R_{8r}\beta_2+R_{8i}\beta_1)/4
\end{aligned}$$

Appendix C: Case of 3-Queues

In the case of $N=3$, the parameters β_1 and β_2 are given by

$$\beta_1 = \frac{9\Lambda\cos(\omega_c\Delta_c)-3\Lambda^2\Delta_c}{9+\Lambda^2\Delta_c^2-6\Lambda\Delta_c\cos(\omega_c\Delta_c)} \tag{6.109}$$

$$\beta_2 = \frac{-9\Lambda\sin(\omega_c\Delta_c)}{9+\Lambda^2\Delta_c^2-6\Lambda\Delta_c\cos(\omega_c\Delta_c)} \tag{6.110}$$

The parameters of the modulations equations (5.75), (5.76) and (5.77) are

$$\begin{aligned}
S_1 &= -\frac{\beta_2}{3}\omega_c\ ;\ S_2=\frac{\beta_1}{72}(1+2H_0+2H_r)-\frac{\beta_2 H_i}{36}\ ;\ S_3=\frac{\beta_1}{108}(1+6H_r)-\frac{\beta_2 H_i}{18}\\
S_4 &= \frac{\beta_1 H_i}{36}-\frac{\beta_2}{216}(1+6H_0-6H_r)=M_3-M_2\ ;\ S_5=\frac{\beta_1}{216}(1+6H_0-6H_r)+\frac{\beta_2 H_i}{36}\\
M_1 &= \frac{\beta_1}{3}\omega_c\ ;\ M_2=\frac{\beta_1}{36}H_i+\frac{\beta_2}{72}(1+2H_0+2H_r)\ ;\ M_3=\frac{\beta_1}{18}H_i+\frac{\beta_2}{108}(1+6H_r)
\end{aligned} \tag{6.111}$$

Appendix D: Stability of the periodic solutions

The sign of the eigenvalues of the Jacobian matrix $\mathbb{J}$ give information about the linear stability of equilibria. Hence, an equilibrium is stable if all the eigenvalues of its $\mathbb{J}$ have negative real parts. It is unstable if at least one of the eigenvalues has a positive real part. The three eigenvalues of the Jacobian matrix of Eqs. (5.75), (5.76) and (5.77) of the fixed points $\mathcal{P}_1, \mathcal{P}_2$ and $\mathcal{P}_3$ given in Eqs. (5.78), (5.79) and (5.80) are given by

- for $\mathcal{P}_1$:

$$\left(-2\delta S_1, \frac{2\delta S_1 S_5}{S_3+S_5}, \frac{-2\delta S_1(S_2-S_3-S_5)}{S_3+S_5}\right)$$

.

- for $\mathcal{P}_2$:
$$\left(-2\delta S_1, \frac{6\delta S_1 S_5}{2S_2+S_3+S_5}, \frac{-2\delta S_1(S_2-S_3-S_5)}{2S_2+S_3+S_5}\right)$$
.
- for $\mathcal{P}_3$:
$$\left(-2\delta S_1, \frac{\delta S_1(\sigma_1+2\sqrt{\sigma_2})}{S_2+2S_3-S_5}, \frac{\delta S_1(\sigma_1-2\sqrt{\sigma_2})}{S_2+2S_3-S_5}\right)$$
.

where $\sigma_1 = -2S_2+2S_3-4S_5$ and $\sigma_2 = (S_2-S_3-S_5)^2-9S_4^2$.
For the numerical values considered in our case i.e., $\lambda = 10$ and $\mu = 1$, the eigenvalues of the Jacobian matrix are: for $\mathcal{P}_1$: $(1.679\delta, -3.345\delta, 0)$, for $\mathcal{P}_2$: $(1.679\delta, -3.345\delta, 0)$ and for $\mathcal{P}_3$: $(-3.345\delta, (-3.370+i0.965)\delta, (-3.370-i0.965)\delta)$. Consequently, the only stable equilibrium is $\mathcal{P}_3$.

Appendix E

In the case of three queues, modulation equations of the phases θ_2 and θ_3 are given by

$$\begin{aligned} a_2\dot{\theta}_2 &= M_1\delta a_2 + M_2 a_2^3 + M_3 a_2 a_3^2 + \left(-M_2\cos(\Psi)+S_5\sin(\Psi)\right)a_2^2 a_3 \\ &+ \left(-S_4\cos(2\Psi)-S_5\sin(2\Psi)\right)a_2 a_3^2 \end{aligned} \quad (6.112)$$

$$\begin{aligned} a_3\dot{\theta}_3 &= M_1\delta a_3 + M_2 a_3^3 + M_3 a_2^2 a_3 + \left(-M_2\cos(\Psi)-S_5\sin(\Psi)\right)a_2 a_3^2 \\ &+ \left(-S_4\cos(2\Psi)+S_5\sin(2\Psi)\right)a_2^2 a_3 \end{aligned} \quad (6.113)$$

If both a_2 and a_3 are not trivial, then we define the phases difference by $\Psi = \theta_2 - \theta_3$. It is governed by the following equation

$$\dot{\Psi} = -S_4\left(1-\cos(2\Psi)\right)(a_2^2-a_3^2) + 2S_5 a_2 a_3\sin(\Psi) - S_5(a_2^2+a_3^2)\sin(2\Psi) \quad (6.114)$$

In the particular case where $a_2 = a_3 = a_3^*$, we get

$$\dot{\Psi} = 2S_5 a_3^{*2}\sin(\Psi)\left(1-2\cos(\Psi)\right) \quad (6.115)$$

The Ψ will converge to the stable equilibrium $\Psi_s = \pi/3$, consequently, the phases modulations equations (6.112) and (6.113) become

$$\dot{\theta}_2 = M_1\delta + \left(\frac{M_2}{2}+M_3+\frac{S_4}{2}\right)a_3^{*2} \quad (6.116)$$

$$\dot{\theta}_3 = M_1\delta + \left(\frac{M_2}{2}+M_3+\frac{S_4}{2}\right)a_3^{*2} \quad (6.117)$$

The phases θ_2 and θ_3 are given by

$$\theta_2(t) = \left(\delta M_1 + \left(M_2+2M_3+S_4\right)\frac{a_3^{*2}}{2}\right)t + \theta_{20} \quad (6.118)$$

$$\theta_3(t) = \left(\delta M_1 + \left(M_2+2M_3+S_4\right)\frac{a_3^{*2}}{2}\right)t + \theta_{30} \quad (6.119)$$

Solutions of lengths differences given by the MSM up to the order $\mathcal{O}(1)$ are given by

$$D_2(t) = a_3^* \cos(\Omega t + \theta_{20}) + \mathcal{O}(\varepsilon) \quad (6.120)$$

$$D_3(t) = a_3^* \cos(\Omega t + \theta_{30}) + \mathcal{O}(\varepsilon) \quad (6.121)$$

where the fundamental frequency of $D_2(t)$ and $D_3(t)$ is given by

$$\Omega = \omega_c + \left(\delta M_1 + (M_2 + 2M_3 + S_4) \frac{a_3^{*2}}{2} \right). \quad (6.122)$$

References

[1] Gad Allon and Achal Bassamboo. The impact of delaying the delay announcements. *Operations research*, 59(5):1198–1210, 2011.

[2] Gad Allon, Achal Bassamboo, and Itai Gurvich. "we will be right with you": Managing customer expectations with vague promises and cheap talk. *Operations research*, 59(6): 1382–1394, 2011.

[3] Mor Armony and Constantinos Maglaras. On customer contact centers with a call-back option: Customer decisions, routing rules, and system design. *Operations Research*, 52 (2):271–292, 2004.

[4] Mor Armony, Nahum Shimkin, and Ward Whitt. The impact of delay announcements in many-server queues with abandonment. *Operations Research*, 57(1):66–81, 2009.

[5] Farshid Maghami Asl and A Galip Ulsoy. Analysis of a system of linear delay differential equations. *Journal of Dynamic Systems, Measurement, and Control*, 125(2):215–223, 2003.

[6] Athanassios N Avramidis and Pierre L'Ecuyer. Modeling and simulation of call centers. In *Proceedings of the Winter Simulation Conference, 2005.*, pages 9–pp. IEEE, 2005.

[7] Achal Bassamboo and Rouba Ibrahim. A general framework to compare announcement accuracy: Static vs les-based announcement. *Working Paper.*, 2018.

[8] Jing Dong, Elad Yom-Tov, and Galit B Yom-Tov. The impact of delay announcements on hospital network coordination and waiting times. *Management Science*, 65(5):1969–1994, 2019.

[9] Pengfei Guo and Paul Zipkin. Analysis and comparison of queues with different levels of delay information. *Management Science*, 53(6):962–970, 2007.

[10] Pengfei Guo and Paul Zipkin. The impacts of customers'delay-risk sensitivities on a queue with balking. *Probability in the engineering and informational sciences*, 23(03): 409–432, 2009.

[11] Jack K Hale. Functional differential equations. In *Analytic theory of differential equations*, pages 9–22. Springer, 1971.

[12] Refael Hassin. Information and uncertainty in a queuing system. *Probability in the Engineering and Informational Sciences*, 21(03):361–380, 2007.

[13] Rouba Ibrahim. Sharing delay information in service systems: a literature survey. *Queueing Systems*, 89(1-2):49–79, 2018.

[14] Rouba Ibrahim and Ward Whitt. Real-time delay estimation in overloaded multiserver queues with abandonments. *Management Science*, 55(10):1729–1742, 2009.

[15] Rouba Ibrahim, Mor Armony, and Achal Bassamboo. Does the past predict the future? the case of delay announcements in service systems. *Management Science*, 63(6):1762–1780, 2017.

[16] Otis B Jennings and Jamol Pender. Comparisons of ticket and standard queues. *Queueing Systems*, 84(1-2):145–202, 2016.

[17] Oualid Jouini, Yves Dallery, and Zeynep Akşin. Queueing models for full-flexible multi-class call centers with real-time anticipated delays. *International Journal of Production Economics*, 120(2):389–399, 2009.

[18] Oualid Jouini, Zeynep Aksin, and Yves Dallery. Call centers with delay information: Models and insights. *Manufacturing & Service Operations Management*, 13(4): 534–548, 2011.

[19] Shamping L.F. and Thompson S. Solving DDEs in Matlab. *Applied Numerical Mathematics*, 37(4):441–458, March 2001.

[20] David Lipshutz and Ruth J Williams. Existence, uniqueness, and stability of slowly oscillating periodic solutions for delay differential equations with nonnegativity constraints. *SIAM Journal on Mathematical Analysis*, 47(6):4467–4535, 2015.

[21] Ali H Nayfeh. *Perturbation methods*. John Wiley & Sons, 2008.

[22] Ali Hasan Nayfeh, Dean T Mook, and P Holmes. Nonlinear oscillations, 1980.

[23] Samantha Nirenberg, Andrew Daw, and Jamol Pender. The impact of queue length rounding and delayed app information on disney world queues. In *2018 Winter Simulation Conference (WSC)*, pages 3849–3860. IEEE, 2018.

[24] Sophia Novitzky, Jamol Pender, Richard Rand, and Elizabeth Wesson. Limiting the oscillations in queues with delayed information through a novel type of delay announcement. *arXiv preprint arXiv:1902.07617*, 2019.

[25] Sophia Novitzky, Jamol Pender, Richard H Rand, and Elizabeth Wesson. Nonlinear dynamics in queueing theory: Determining the size of oscillations in queues with delay. *SIAM Journal on Applied Dynamical Systems*, 18(1):279–311, 2019.

[26] Jamol Pender, Richard H Rand, and Elizabeth Wesson. Queues with choice via delay differential equations. *International Journal of Bifurcation and Chaos*, 27(04):1730016, 2017.

[27] Jamol Pender, Richard H Rand, and Elizabeth Wesson. An analysis of queues with delayed information and time-varying arrival rates. *Nonlinear Dynamics*, 91(4):2411–2427, 2018.

[28] Jamol Pender, Richard Rand, and Elizabeth Wesson. A stochastic analysis of queues with customer choice and delayed information. *Mathematics of Operations Research To Appear*, 2019.

[29] Gaurav Raina and Damon Wischik. Buffer sizes for large multiplexers: Tcp queueing theory and instability analysis. In *Next Generation Internet Networks, 2005*, pages 173–180. IEEE, 2005.

[30] Richard Rand. Differential-delay equations. In *Complex Systems*, pages 83–117. Springer, 2011.

[31] Aditya Shah, Anders Wikum, and Jamol Pender. Using simulation to study the last to enter service delay announcement in multiserver queues with abandonment. In *2019 Winter Simulation Conference (WSC)*, pages 2595–2605. IEEE, 2019.

[32] Shuang Tao and Jamol Pender. A stochastic analysis of bike sharing systems. *arXiv preprint arXiv:1708.08052*, 2017.

[33] Shuang Tao and Jamol Pender. The impact of smartphone apps on bike sharing systems. *arXiv preprint arXiv:2004.10008*, 2020.

[34] Mamadou Thiongane, Wyean Chan, and Pierre L'Ecuyer. Waiting time predictors for multi-skill call centers. In *2015 Winter Simulation Conference (WSC)*, pages 3073–3084. IEEE, 2015.

[35] Mamadou Thiongane, Wyean Chan, and Pierre l'Ecuyer. New history-based delay predictors for service systems. In *2016 Winter Simulation Conference (WSC)*, pages 425–436. IEEE, 2016.

[36] Mamadou Thiongane, Wyean Chan, and Pierre L'Ecuyer. Delay predictors in multi-skill call centers: An empirical comparison with real data. In *International Conference on Operations Research and Enterprise Systems: ICORES*, 2020.

[37] Ward Whitt. Improving service by informing customers about anticipated delays. *Management science*, 45(2):192–207, 1999.